

PROBING THE SUPERSYMMETRY-MASS SCALE WITH F-TERM HYBRID INFLATION

G. LAZARIDES¹ AND C. PALLIS²

¹*School of Electrical & Computer Engineering, Faculty of Engineering,
Aristotle University of Thessaloniki, GR-541 24 Thessaloniki, GREECE*
e-mail address: glazarid@gen.auth.gr

²*Laboratory of Physics, Faculty of Engineering,
Aristotle University of Thessaloniki, GR-541 24 Thessaloniki, GREECE*
e-mail address: kpallis@gen.auth.gr

ABSTRACT: We consider F-term hybrid inflation and supersymmetry breaking in the context of a model which largely respects a global $U(1)$ R symmetry. The Kähler potential parameterizes the Kähler manifold with an enhanced $U(1) \times (SU(1,1)/U(1))$ symmetry, where the scalar curvature of the second factor is determined by the achievement of a supersymmetry-breaking de Sitter vacuum without ugly tuning. The magnitude of the emergent soft tadpole term for the inflaton can be adjusted in the range $(1.2 - 460)$ TeV – increasing with the dimensionality of the representation of the waterfall fields – so that the inflationary observables are in agreement with the observational requirements. The mass scale of the supersymmetric partners turns out to lie in the region $(0.09 - 253)$ PeV which is compatible with high-scale supersymmetry and the results of LHC on the Higgs boson mass. The μ parameter can be generated by conveniently applying the Giudice-Masiero mechanism and assures the out-of-equilibrium decay of the R saxion at a low reheating temperature $T_{\text{rh}} \leq 163$ GeV.

PACs numbers: 98.80.Cq, 12.60.Jv

I. INTRODUCTION

Among the various inflationary models – for reviews see Refs. [1, 2] –, the simplest and most well-motivated one is undoubtedly the *F-term hybrid inflation* (FHI) model [3]. It is tied to a renormalizable superpotential uniquely determined by a global $U(1)$ R symmetry, it does not require fine tuned parameters and transplanckian inflaton values, and it can be naturally followed by a *Grand Unified Theory* (GUT) phase transition – see, e.g., Refs. [4–6]. In the original implementation of FHI [3], the slope of the inflationary path which is needed to drive the inflaton towards the *Supersymmetric* (SUSY) vacuum is exclusively provided by the inclusion of *radiative corrections* (RCs) in the tree level (classically flat) inflationary potential. This version of FHI is considered as strongly disfavored by the *Planck* data [7] fitted to the standard power-law cosmological model with *Cold Dark Matter* (CDM) and a cosmological constant (Λ CDM). A more complete treatment, though, incorporates also corrections originating from *supergravity* (SUGRA) which depend on the adopted Kähler potential [8–11] as well as soft SUSY-breaking terms [12–17]. Mildly tuning the parameters of the relevant terms, we can achieve [18] mostly hilltop FHI fully compatible with the data [7, 19, 20] – observationally acceptable implementations of FHI can also be achieved by invoking a two-step inflationary scenario [21] or a specific generation [5, 22, 23] of the μ term of the *Minimal Supersymmetric Standard Model* (MSSM).

Out of the aforementioned realizations of FHI we focus here on the “tadpole-assisted” one [14, 15] in which the suitable inflationary potential is predominantly generated by the cooperation of the RCs and the soft SUSY-breaking tadpole term. A crucial ingredient for this is the specification of a convenient SUSY-breaking scheme – see, e.g., Refs. [23–27]. Here, we extend the formalism of FHI to encompass SUSY breaking by imposing a mildly violated R symmetry introduced in Ref. [28]. Actually, it acts as a junction mechanism of the (visible) *inflationary sector* (IS) and the *hidden sector*

(HS). A first consequence of this combination is that the R charge $2/\nu$ of the goldstino superfield – which is related to the geometry of the HS – is constrained to values with $0 < \nu < 1$. A second byproduct is that SUSY breaking is achieved not only in a Minkowski vacuum, as in Ref. [28], but also in a *de Sitter* (dS) one which allows us to control the notorious *Dark Energy* (DE) problem by mildly tuning a single superpotential parameter to a value of order 10^{-12} . A third consequence is the stabilization [24–27] of the sgoldstino to low values during FHI. Selecting minimal Kähler potential for the inflaton and computing the suppressed contribution of the sgoldstino to the mass squared of the inflaton, we show that the η -problem of FHI can be elegantly resolved. After these arrangements, the imposition of the inflationary requirements may restrict the magnitude of the naturally induced tadpole term which is a function of the inflationary scale M and the dimensionality N_G of the representation of the waterfall fields. The latter quantity depends on the GUT gauge symmetry \mathbb{G} in which FHI is embedded. We exemplify our proposal by considering three possible \mathbb{G} ’s which correspond to the values $N_G = 1, 2$, and 10. The analysis for the two latter N_G values is done for the first time. We find that the required magnitude of the tadpole term increases with N_G .

For $N_G = 1$ the scale of formation of the $B - L$ *cosmic strings* (CSs) fits well with the bound [29] induced by the observations [19] on the anisotropies of the *cosmic microwave background* (CMB) radiation. These $B - L$ CSs are rendered metastable, if the $U(1)_{B-L}$ symmetry is embedded in a GUT based on a group with higher rank such as $SO(10)$. In such a case, the CS network decays generating a stochastic background of gravitational waves that may interpret [30, 31] the recent data from NANOGrav [32] and other pulsar timing array experiments [33] – see also Ref. [34].

Finally, a solution to the μ problem of MSSM – for an updated review see Ref. [35] – may be achieved by suitably applying [28] the Giudice-Masiero mechanism [36, 37]. Contrary to similar attempts [22, 23], the μ term here plays no

role during FHI. This term assures [38–42] the timely decay of the sgoldstino (or R saxion), which dominates the energy density of the universe, before the onset of the *Big Bang Nucleosynthesis* (BBN) at cosmic temperature $(2 - 4)$ MeV [43]. In a portion of the parameter space with $3/4 < \nu < 1$ non-thermal production of gravitinos (\tilde{G}) is prohibited and so the moduli-induced \tilde{G} problem [44] can be easily eluded. Finally, our model sheds light to the rather pressing problem of the determination of the SUSY mass scale \tilde{m} which remains open to date [45] due to the lack of any SUSY signal in LHC – for similar recent works see Refs. [46–51]. In particular, our setting predicts \tilde{m} close to the PeV scale and fits well with high-scale SUSY and the Higgs boson mass discovered at LHC [52] if we assume a relatively low $\tan\beta$ and stop mixing [53].

We describe below how we can interconnect the inflationary and the SUSY-breaking sectors of our model in Sec. II. Then, we propose a resolution to the μ problem of MSSM in Sec. III and study the reheating process in Sec. IV. We finally present our results in Sec. VI confronting our model with a number of constraints described in Sec. V. Our conclusions are discussed in Sec. VII. General formulas for the SUGRA-induced corrections to the potential of FHI are arranged in the Appendix.

II. LINKING FHI WITH THE SUSY BREAKING SECTOR

As mentioned above, our model consists of two sectors: the HS responsible for the F-term (spontaneous) SUSY breaking and the IS responsible for FHI. In this Section we first – in Sec. II A – specify the conditions under which the coexistence of both sectors can occur and then – in Sec. II B – we investigate the vacua of the theory. Finally, we derive the inflationary potential in Sec. II C.

A. Set-up

Here we determine the particle content, the superpotential, and the Kähler potential of our model. These ingredients are presented in Secs. II A 1, II A 2, and II A 3. Then in Sec. II A 4 we present the general structure of the SUGRA scalar potential which governs the evolution of the HS and IS.

1. Particle Content

As well-known, FHI can be implemented by introducing three superfields $\bar{\Phi}$, Φ , and S . The two first are left-handed chiral superfields oppositely charged under a gauge group \mathbb{G} whereas the latter is the inflaton and is a \mathbb{G} -singlet left-handed chiral superfield. Singlet under \mathbb{G} is also the SUSY breaking (goldstino) superfield Z .

In this work we identify \mathbb{G} with three possible gauge groups with different dimensionality N_G of the representations to which $\bar{\Phi}$ and Φ belong. Namely, we consider

- $\mathbb{G} = \mathbb{G}_{B-L}$ with $\mathbb{G}_{B-L} = \mathbb{G}_{SM} \times U(1)_{B-L}$, where \mathbb{G}_{SM} is the Standard Model gauge group. In this case Φ and $\bar{\Phi}$ belong [14] to the $(\mathbf{1}, \mathbf{1}, 0, -1)$ and $(\mathbf{1}, \mathbf{1}, 0, 1)$ representation of \mathbb{G}_{B-L} respectively and so $N_G = 1$.
- $\mathbb{G} = \mathbb{G}_{LR}$ with $\mathbb{G}_{LR} = SU(3)_C \times SU(2)_L \times SU(2)_R \times U(1)_{B-L}$. In this case Φ and $\bar{\Phi}$ belong [4, 5] to the $(\mathbf{1}, \mathbf{1}, \mathbf{2}, -1)$ and $(\mathbf{1}, \mathbf{1}, \bar{\mathbf{2}}, 1)$ representation of \mathbb{G}_{LR} respectively and so $N_G = 2$.
- $\mathbb{G} = \mathbb{G}_{5X}$ with $\mathbb{G}_{5X} = SU(5) \times U(1)_X$, the gauge group of the flipped $SU(5)$ model. In this case Φ and $\bar{\Phi}$ belong [6] to the $(\mathbf{10}, 1)$ and $(\bar{\mathbf{10}}, -1)$ representation of \mathbb{G}_{5X} respectively and so $N_G = 10$.

In the cases above, we assume that \mathbb{G} is completely broken via the *vacuum expectation values* (VEVs) of Φ and $\bar{\Phi}$ to \mathbb{G}_{SM} . No magnetic monopoles are generated during this GUT transition, in contrast to the cases where $\mathbb{G} = SU(4)_C \times SU(2)_L \times SU(2)_R$, $SU(5)$, or $SO(10)$. The production of magnetic monopole can be avoided, though, even in these groups if we adopt the shifted [54] or smooth [55] variants of FHI.

2. Superpotential

The superpotential of our model has the form

$$W = W_I(S, \Phi, \bar{\Phi}) + W_H(Z) + W_{GH}(Z, \bar{\Phi}, \Phi), \quad (1)$$

where the subscripts “I” and “H” stand for the IS and HS respectively. The three parts of W are specified as follows:

- a. W_I is the IS part of W written as [3]

$$W_I = \kappa S (\bar{\Phi}\Phi - M^2), \quad (2a)$$

where κ and M are free parameters which may be made positive by field redefinitions.

- b. W_H is the HS part of W which reads [28]

$$W_H = mm_P^2 (Z/m_P)^\nu. \quad (2b)$$

Here $m_P = 2.4 \times 10^{18}$ GeV is the reduced Planck mass, m is a positive free parameter with mass dimensions, and ν is an exponent which may, in principle, acquire any real value if W_H is considered as an effective superpotential valid close to the non-zero vacuum value of Z . We will assume though that the effective superpotential is such that only positive powers of Z appear.

- c. W_{GH} is an unavoidable term – see below – which mixes Z with $\bar{\Phi}$ and Φ and has the form

$$W_{GH} = -\lambda m_P (Z/m_P)^\nu \bar{\Phi}\Phi, \quad (2c)$$

with λ a real coupling constant.

W is fixed by imposing an R symmetry under which W and the various superfields have the following R characters

$$R(W) = R(S) = 2, \quad R(Z) = 2/\nu \quad \text{and} \quad R(\bar{\Phi}\Phi) = 0. \quad (3)$$

As we will see below, we confine ourselves in the range $3/4 < \nu < 1$. We assume that W is holomorphic in S and so S

appears with positive integer exponents ν_s . Mixed terms of the form $S^{\nu_s} Z^{\nu_z}$ must obey the R symmetry and thus

$$\nu_s + \nu_z/\nu = 1 \Rightarrow \nu_z = (1 - \nu_s)\nu, \quad (4)$$

leading to negative values of ν_z . Therefore no such mixed terms appear in the superpotential.

3. Kähler Potential

The Kähler potential has two contributions

$$K = K_I(S, \Phi, \bar{\Phi}) + K_H(Z), \quad (5)$$

which are specified as follows:

a. K_I is the part of K which depends on the fields involved in FHI – cf. Eq. (2a). We adopt the simplest possible form

$$K_I = |S|^2 + |\Phi|^2 + |\bar{\Phi}|^2, \quad (6a)$$

which parameterizes the $U(1)_S \times U(1)_\Phi \times U(1)_{\bar{\Phi}}$ Kähler manifold – the indices here indicate the moduli which parameterize the corresponding manifolds.

b. K_H is the part of K devoted to the HS. We adopt the form introduced in Ref. [28] where

$$K_H = Nm_P^2 \ln \left(1 + \frac{|Z|^2 - k^2 Z_-^4/m_P^2}{Nm_P^2} \right), \quad (6b)$$

with $Z_\pm = Z \pm Z^*$. Here, k is a parameter which mildly violates R symmetry endowing R axion with phenomenologically acceptable mass. Despite the fact that there is no string-theoretical motivation for K_H , we consider it as an interesting phenomenological option since it ensures a vanishing potential energy density in the vacuum without tuning for

$$N = \frac{4\nu^2}{3 - 4\nu} \quad (7)$$

when ν is confined to the following ranges

$$\frac{3}{4} < \nu < \frac{3}{2} \text{ for } N < 0 \text{ and } \nu < \frac{3}{4} \text{ for } N > 0. \quad (8)$$

As we will see below the same $\nu - N$ relation assists us to obtain a dS vacuum of the whole field system with tunable cosmological constant. Our favored ν range will finally be $3/4 < \nu < 1$. This range is included in Eq. (8) for $N < 0$. Therefore, K_H parameterizes the $(SU(1,1)/U(1))_Z$ hyperbolic Kähler manifold. The total K in Eq. (5) enjoys an enhanced symmetry for the S and Z fields, namely $U(1)_S \times (SU(1,1)/U(1))_Z$. Thanks to this symmetry, mixing terms of the form $S^{\nu_s} Z^{\nu_z}$ can be ignored although they may be allowed by the R symmetry for $\tilde{\nu}_z = \nu\tilde{\nu}_s$.

4. SUGRA Potential

Denoting the various superfields of our model as $X^\alpha = S, Z, \Phi, \bar{\Phi}$ and employing the same symbol for their complex scalar components, we can find the F-term (tree level)

SUGRA scalar potential V_F from W in Eq. (1) and K in Eq. (5) by applying the standard formula [56]

$$V_F = e^{K/m_P^2} \left(K^{\alpha\bar{\beta}} D_\alpha W D_{\bar{\beta}} W^* - 3|W|^2/m_P^2 \right), \quad (9)$$

with $K_{\alpha\bar{\beta}} = \partial_{X^\alpha} \partial_{X^*\bar{\beta}} K$, $K^{\bar{\beta}\alpha} K_{\alpha\bar{\gamma}} = \delta_{\bar{\gamma}}^{\bar{\beta}}$ and

$$D_\alpha W = \partial_{X^\alpha} W + W \partial_{X^\alpha} K/m_P^2. \quad (10)$$

Thanks to the simple form of K in Eqs. (5), (6a), and (6b), the Kähler metric $K_{\alpha\bar{\beta}}$ has diagonal form with only one non-trivial element

$$K_{ZZ^*} = (Nm_P^4 - k^2 Z_-^4 + m_P^2 |Z|^2)^{-2} m_P^2 N \times (m_P^6 N + 12Nk^2 m_P^4 Z_-^2 + 4k^4 Z_-^6 + 3k^2 m_P^2 Z_-^2 Z_+^2). \quad (11)$$

The resulting V_F can be written as

$$V_F = e^{\frac{K}{m_P^2}} \left(|v_S|^2 + |v_\Phi|^2 + |v_{\bar{\Phi}}|^2 + K_{ZZ^*}^{-1} |v_Z|^2 - 3|v_W|^2 \right), \quad (12)$$

where the individual contributions are

$$v_S = \kappa(\bar{\Phi}\Phi - M^2) (|S/m_P|^2 + 1) - S^* Z^\nu / m_P^{\nu+1} (mm_P - \lambda\bar{\Phi}\Phi), \quad (13a)$$

$$v_\Phi = \kappa S (M^2 m_P^{-2} \Phi^* - \bar{\Phi}(|\Phi|^2 m_P^{-2} + 1)) + Z^\nu m_P^{1-\nu} (\lambda\bar{\Phi}(|\Phi/m_P|^2 + 1) - mm_P^{-1} \Phi^*), \quad (13b)$$

$$v_Z = \nu(Z/m_P)^{\nu-1} (mm_P - \lambda\bar{\Phi}\Phi) + N (Z^* m_P^2 - 4k^2 Z_-^3) (Nm_P^4 - k^2 Z_-^4 + |Z|^2 m_P^2)^{-1} \times ((Z/m_P)^\nu (mm_P^2 - \lambda\bar{\Phi}\Phi) + \kappa S(\bar{\Phi}\Phi - M^2)), \quad (13c)$$

$$v_W = \kappa S m_P^{-1} (\bar{\Phi}\Phi - M^2) + Z^\nu m_P^{-\nu} (mm_P - \lambda\bar{\Phi}\Phi). \quad (13d)$$

Note that $v_{\bar{\Phi}}$ is obtained from v_Φ by interchanging Φ with $\bar{\Phi}$. Obviously, Eq. (7) was not imposed in the formulas above.

D-term contributions to the total SUGRA scalar potential arise only from the \mathbb{G} non-singlet fields. They take the form

$$V_D = \frac{g^2}{2} (|\Phi|^2 - |\bar{\Phi}|^2)^2, \quad (14)$$

where g is the gauge coupling constant of \mathbb{G} . During FHI and at the SUSY vacuum we confine ourselves along the D-flat direction

$$|\bar{\Phi}| = |\Phi|, \quad (15)$$

which assures that $V_D = 0$.

B. SUSY and \mathbb{G} Breaking Vacuum

As we can verify numerically, V_F in Eq. (12) is minimized at the \mathbb{G} -breaking vacuum

$$|\langle \Phi \rangle| = |\langle \bar{\Phi} \rangle| = M. \quad (16)$$

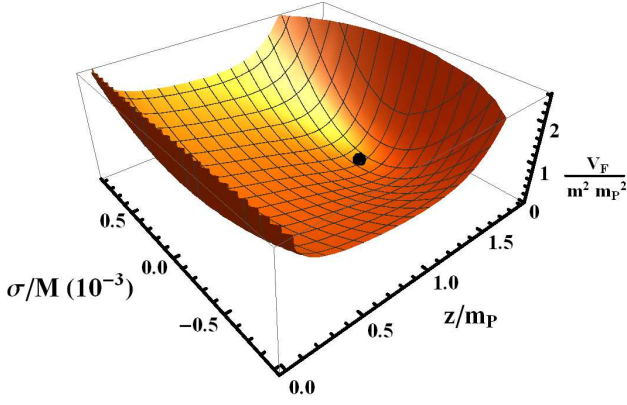


FIG. 1: The (dimensionless) SUGRA potential $V_F/m^2 m_P^2$ in Eq. (18) as a function of z and σ for the inputs shown in column B of Table I. The location of the dS vacuum in Eq. (22) is also depicted by a thick point.

It has also a stable valley along $\langle \theta \rangle = 0$ and $\langle \theta_S/m_P \rangle = \pi$, with these fields defined by

$$Z = (z + i\theta)/\sqrt{2} \text{ and } S = \sigma e^{i\theta_S/m_P}/\sqrt{2}. \quad (17)$$

As we will see below, $\theta_S/m_P = \pi$ holds during FHI and we assume that it is also valid at the vacuum. Substituting Eq. (17) in Eq. (12), we obtain the partially minimized V_F as a function of z and σ , i.e.,

$$V_F(z, \sigma) = 2^{-(\nu+1)} e^{\langle K_H \rangle / m_P^2} \left((\lambda M^2 - m m_P)^2 (z/m_P)^{2\nu} \left(\frac{(2N m_P^2 \nu + (\nu + N) z^2)^2}{N^2 z^2 m_P^2} - 6 + \frac{\sigma^2}{m_P^2} \right) + \left(2^{\frac{1+\nu}{2}} \kappa M \sigma + \frac{(2M(\lambda(M^2 + m_P^2) - m m_P) z^\nu)^2}{m_P^{\nu+1}} \right)^2 \right). \quad (18)$$

The minimization of the last term implies

$$\sigma = -2^{(1-\nu)/2} (\lambda(M^2 + m_P^2) - m m_P) z^\nu / m_P^{(\nu+1)}, \quad (19)$$

whereas imposing the condition in Eq. (7) we obtain [28]

$$\frac{(2N m_P^2 \nu + (\nu + N) z^2)^2}{N^2 z^2 m_P^2} - 6 = \frac{(3z^2 - 8\nu m_P^2)^2}{16\nu^2 z^2 m_P^2}. \quad (20)$$

Substituting the two last relations into Eq. (18) we arrive at the result

$$V_F(z) = e^{\langle K_H \rangle / m_P^2} (\lambda M^2 - m m_P)^2 z^{2\nu} \left(\frac{((\lambda(M^2 + m_P^2) - m m_P)^2 z^{2\nu} + \frac{(8\nu^2 m_P^2 - 3z^2)^2}{2^{5+\nu} \nu^2 z^2 m_P^{2(\nu+1)}})}{2^{2\nu} \kappa^2 m_P^{4(1+\nu)}} \right), \quad (21)$$

which is minimized *with respect to* (w.r.t.) σ too. From the last expression we can easily find that z acquires the VEV

$$\langle z \rangle = 2\sqrt{2/3} |\nu| m_P, \quad (22)$$

which yields the constant potential energy density

$$\langle V_F \rangle = \left(\frac{16\nu^4}{9} \right)^\nu \left(\frac{\lambda M^2 - m m_P}{\kappa m_P^2} \right)^2 \omega^N \times (\lambda(M^2 + m_P^2) - m m_P)^2, \quad (23)$$

with

$$\omega = e^{\langle K_H \rangle / N m_P^2} \simeq 2(3 - 2\nu)/3, \quad (24)$$

given that $M \ll m_P$. Tuning λ to a value $\lambda \sim m/m_P \simeq 10^{-12}$ we can obtain a post-inflationary dS vacuum which corresponds to the current DE density parameter. By virtue of Eq. (19), we also obtain $\langle \sigma \rangle \simeq 0$.

The gravitino (\tilde{G}) acquires mass [56]

$$m_{3/2} = \langle e^{\frac{\langle K_H \rangle}{2m_P^2}} W_H \rangle \simeq 2^\nu 3^{-\nu/2} |\nu|^\nu m \omega^{N/2}. \quad (25a)$$

Deriving the mass-squared matrix of the field system $S - \Phi - \bar{\Phi} - Z$ at the vacuum we find the residual mass spectrum of the model. Namely, we obtain a common mass for the IS

$$m_I = e^{\frac{\langle K_H \rangle}{2m_P^2}} \sqrt{2} (\kappa^2 M^2 + (4\nu^2/3)^\nu (1 + 4M^2/m_P^2) m^2)^{\frac{1}{2}}, \quad (25b)$$

where the second term arises due to the coexistence of the IS with the HS – cf. Ref. [14]. We also obtain the (canonically normalized) sgoldstino (or R saxion) and the pseudo-sgoldstino (or R axion) with respective masses

$$m_z \simeq \frac{3\omega}{2\nu} m_{3/2} \text{ and } m_\theta \simeq 12\kappa\omega^{\frac{3}{2}} m_{3/2}. \quad (25c)$$

Comparing the last formulas with the ones obtained in the absence of the IS [28] we infer that no mixing appears between the IS and the HS. As in the “isolated” case of Ref. [28] the role of k in Eq. (6b) remains crucial in providing θ with a mass. Some representative values of the masses above are arranged in Table I for specific κ, ν , and k values and for the three G ’s considered in Sec. II A 1. We employ values for M and the tadpole parameter a_S compatible with the inflationary requirements exposed in Sec. V – for the definition of a_S see Sec. II C 4. We observe that m_I turns out to be of order 10^{12} GeV – cf. Ref. [14] – whereas $m_{3/2}, m_z$, and m_θ lie in the PeV range. For the selected value $\nu = 7/8 > 3/4$ the phenomenologically desired hierarchy $m_z < 2m_{3/2}$ – see Sec. V – is easily achieved. In the same Table we find it convenient to accumulate the values of some inflationary parameters introduced in Secs. II C 4 and VI and some parameters related to the μ term of the MSSM and the reheat temperature given in Secs. III and IV.

Our analytic findings related to the stabilization of the vacuum in Eqs. (16) and (22) can be further confirmed by Fig. 1, where the dimensionless quantity $V_F/m^2 m_P^2$ in Eq. (18) is plotted as a function of z and σ . We employ the values of the parameters listed in column B of Table I. We see that the dS vacuum in Eq. (22) – indicated by the black thick point – is placed at $(\langle z \rangle, \langle \sigma \rangle) = (1.43 m_P, 0)$ and is stable w.r.t. both directions.

TABLE I: A Case Study Overview

CASE:	A	B	C
INPUT PARAMETERS			
$\kappa = 5 \times 10^{-4}$, $\nu = 7/8$ ($N = -49/8$) and $k = 0.1$			
N_G	1	2	10
M (10^{15} GeV)	1.4	1.9	3.6
m (PeV) ^a	0.5	1.15	6.3
λ (10^{-12})	0.2	1.7	2.6
HS PARAMETERS DURING FHI			
$\langle z \rangle_I$ ($10^{-3} m_P$)	1.1	1.5	2.5
$m_{13/2}$ (TeV)	1.2	2.98	25
m_{1z} (EeV)	0.64	1.1	4.1
$m_{1\theta}$ (EeV)	0.15	0.32	1.2
INFLATIONARY PARAMETERS			
a_S (TeV)	2.63	6.7	56.3
H_I (EeV)	0.25	0.4	1.6
$\sigma_*/\sqrt{2}M$	1.026	1.035	1.067
N_{I*}	40.5	40.8	40.6
Δ_{c*} (%)	2.6	3.5	6.7
$\Delta_{\max*}$ (%)	2.9	3.9	7.3
INFLATIONARY OBSERVABLES			
n_s		0.967	
$-\alpha_s$ (10^{-4})	2.3	2.5	2.9
r (10^{-12})	0.9	3.1	39.7
SPECTRUM AT THE VACUUM			
m_I (10^{12} GeV)	1.8	2.4	4.5
$m_{3/2}$ (PeV)	0.9	2.	11.2
m_z (PeV)	1.3	2.9	16
m_θ (PeV)	0.8	1.8	10
REHEAT TEMPERATURE			
FOR $\mu = \tilde{m}$ ($\lambda_\mu = 0.69$) AND $K = K_1$			
T_{rh} (GeV)	0.07	0.18	2.05

^aRecall that 1 PeV = 10^6 GeV and 1 EeV = 10^9 GeV.

C. Inflationary Period

It is well known [2, 3] that FHI takes place for sufficiently large $|S|$ values along a F- and D- flat direction of the SUSY potential

$$\bar{\Phi} = \Phi = 0, \quad (26)$$

where the potential in global SUSY

$$V_{\text{SUSY}}(\Phi = 0) \equiv V_{I0} = \kappa^2 M^4 \quad (27)$$

provides a constant potential energy density with corresponding Hubble parameter $H_I = \sqrt{V_{I0}/3m_P^2}$. In a SUGRA context, though, we first check – in Sec. IIC 1 – the conditions under which such a scheme can be achieved and then we include a number of corrections described in Secs. IIC 2 and IIC 3 below. The final form of the inflationary potential is given in Sec. IIC 4.

1. Hidden Sector's Stabilization

The implementation of FHI is feasible in our set-up if Z is well stabilized during it. As already emphasized [27], V_{I0} in Eq. (26) is expected to transport the value of Z from the value in Eq. (22) to values well below m_P . To determine these values, we construct the complete expression for V_F in Eq. (12) along the inflationary trough in Eq. (26) and then expand the resulting expression for low S/m_P values, assuming that the $\theta = 0$ direction is stable as in the vacuum. Under these conditions V_F takes the form

$$V_F(z) = e^{\frac{\kappa_H}{m_P^2}} \left(\kappa^2 M^4 + m^2 \frac{z^{2(\nu-1)}(8\nu^2 m_P^2 - 3z^2)^2}{2^{5+\nu} \nu^2 m_P^{2\nu}} \right). \quad (28)$$

The extremum condition obtained for $V_F(z)$ w.r.t. z yields

$$m^2 m_P^{-2\nu} \langle z \rangle_I^{2(\nu-2)} (64\nu^4 m_P^4 - 9\langle z \rangle_I^4) \times \\ (8(1-\nu)\nu^2 m_P^2 + (3-\nu)\langle z \rangle_I^2) = 2^{(7+\nu)} \nu^4 V_{I0}, \quad (29)$$

where the subscript I denotes that the relevant quantity is calculated during FHI. Given that $\langle z \rangle_I/m_P \ll 1$, the equation above implies

$$\langle z \rangle_I \simeq \left(\sqrt{3} \times 2^{\nu/2-1} H_I / m \nu \sqrt{1-\nu} \right)^{1/(\nu-2)} m_P, \quad (30)$$

which is in excellent agreement with its precise numerical value. We remark that $\nu < 1$ assures the existence and the reality of $\langle z \rangle_I$, which is indeed much less than m_P since $H_I/m \ll 1$.

To highlight further this key point of our scenario, we plot in Fig. 2 the quantity $10^5(V_F/\kappa^2 M^4 - 1)$ with V_F given by Eq. (12) for fixed $\Phi = \bar{\Phi} = 0$ – see Eq. (26) – and the remaining parameters listed in column B of Table I. In the left panel we use as free coordinates z and σ with fixed $\theta = 0$. We see that the location of $(\langle z \rangle_I, \sigma_*) = (1.5 \times 10^{-3} m_P, 1.4637M)$, where σ_* is the value of σ when the pivot scale crosses outside the horizon and is indicated by a black thick point, is independent from σ as expected from Eq. (30). In the right panel of this figure we use as coordinates z and θ and fix $\sigma = \sigma_*$. We observe that $(\langle z \rangle_I, \theta) = (1.5 \times 10^{-3} m_P, 0)$ – indicated again by a black thick point – is well stabilized in both directions.

The (canonically normalized) components of sgoldstino acquire masses squared, respectively,

$$m_{1z}^2 \simeq 6(2-\nu)H_I^2 \quad \text{and} \quad m_{1\theta}^2 \simeq 3H_I^2 -$$

$$m^2(8\nu^2 m_P^2 - 3\langle z \rangle_I^2) \frac{4\nu(1-\nu)m_P^2 + (1-96k^2\nu)\langle z \rangle_I^2}{2^{3+\nu}\nu m_P^{2\nu} \langle z \rangle_I^{2(2-\nu)}}, \quad (31a)$$

whereas the mass of \tilde{G} turns out to be

$$m_{13/2} \simeq \left(\nu(1-\nu)^{1/2} m^2/\nu / \sqrt{3} H_I \right)^{\nu/(2-\nu)}. \quad (31b)$$

It is evident from the results above that $m_{1z} \gg H_I$ and therefore $\langle z \rangle_I$ is well stabilized during FHI whereas $m_{1\theta} \simeq H_I$ and

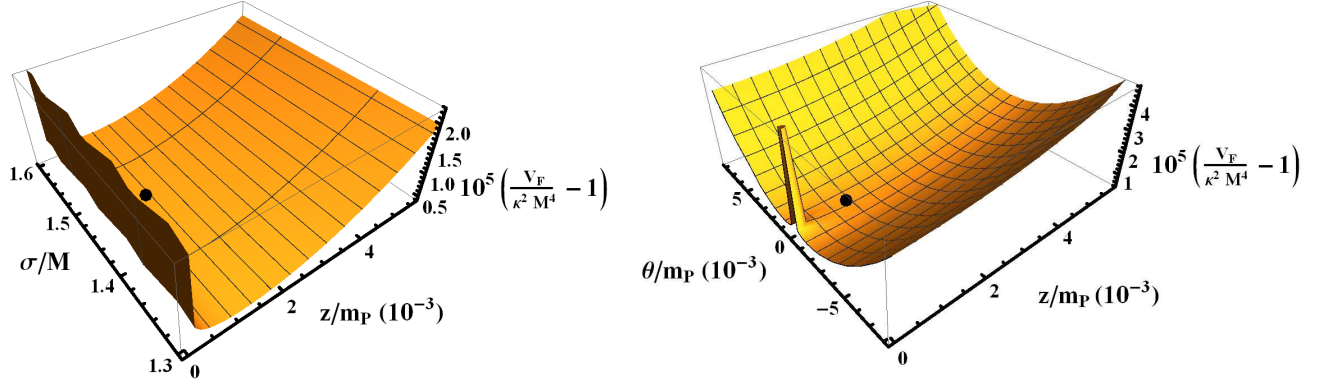


FIG. 2: The SUGRA potential $10^5(V_F/\kappa^2 M^4 - 1)$ in Eq. (12) along the path in Eq. (26) as a function of z and σ for $\theta = 0$ (left panel) or z and θ for $\sigma = \sigma_*$ (right panel). In both cases we take the parameters of column B in Table I. The location of $(\langle z \rangle_I, \sigma_*)$ (left panel) or $(\langle z \rangle_I, 0)$ (right panel) is also depicted by a thick black point.

gets slightly increased as k increases. We do not think that this fact causes any problem with isocurvature perturbations since these can be observationally dangerous only for $m_{I\theta} \ll H_I$. As verified by our numerical results, all the masses above display no S dependence and so they do not contribute to the inclination of the inflationary potential via RCs – see Sec. II C 3 below.

2. SUGRA Corrections

The SUGRA potential in Eq. (9) induces a number of corrections to V_{I0} originating not only from the IS but also from the HS. These corrections are displayed in the Appendix for arbitrary W_H and K_H . If we consider the W_H and K_H in Eqs. (2b) and (6b) respectively, the v 's in Eq. (A.5) are found to be

$$v_1 = 2\kappa M^2 m_{3/2} (2 - \nu - 3\langle z \rangle_I^2 / 8\nu m_P^2), \quad (32a)$$

$$v_2 = \kappa^2 M^4 \langle z \rangle_I^2 / 2m_P^2, \quad (32b)$$

$$v_3 = \kappa M^2 m_{3/2} (1 - \nu - 3\langle z \rangle_I^2 / 8\nu m_P^2), \quad (32c)$$

$$v_4 = \kappa^2 M^4 (1 + \langle z \rangle_I^2 / m_P^2) / 2. \quad (32d)$$

Since $\langle z \rangle_I \ll m_P$ we do not discriminate between κ and its rescaled form following the formulas of the Appendix. Despite the fact that v_2 and v_4 receive contributions from both IS and HS, as noted in the Appendix, here the IS does not participate in v_2 thanks to the selected canonical Kähler potential for the S field in Eq. (6a). This fact together with the smallness of $\langle z \rangle_I^2$ assists us to overcome the notorious η problem of FHI.

3. Radiative Corrections

These corrections originate [3] from a mass splitting in the $\Phi - \bar{\Phi}$ supermultiplets due to SUSY breaking on the inflationary valley. To compute them we work out the mass spectrum

of the fluctuations of the various fields about the inflationary trough in Eq. (26). We obtain $2N_G$ Weyl fermions and $2N_G$ pairs of real scalars with mass squared respectively

$$m_f^2 = \kappa^2 S_\lambda^2 \text{ and } m_\pm^2 = \kappa^2 (S_\lambda^2 \pm M^2) \quad (33)$$

with $S_\lambda = |S| - \lambda \langle Z \rangle_I^\nu m_P^{1-\nu} / \kappa$. SUGRA corrections to these masses are at most of order M^4/m_P^2 and can be safely ignored. Inserting these masses into the well-known Coleman-Weinberg formula, we find the correction

$$V_{RC} = \frac{\kappa^2 N_G}{32\pi^2} V_{I0} \left(\sum_{i=\pm} m_i^4 \ln \frac{m_i^2}{Q^2} - 2m_f^4 \ln \frac{m_f^2}{Q^2} \right), \quad (34)$$

where Q is a renormalization scale. Assuming positivity of m_-^2 , we obtain the lowest possible value S_c of S which assures stability of the direction in Eq. (26). This critical value is equal to

$$|S_c| = M + \lambda \langle Z \rangle_I^\nu m_P^{1-\nu} / \kappa. \quad (35)$$

Needless to say, the mass spectrum and $|S_c|$ deviate slightly from their values in the simplest model of FHI [3] due to the mixing term in W – see Eq. (2c).

4. Inflationary Potential

Substituting Eqs. (32a) – (32d) into V_F in Eq. (A.5), including V_{RC} from Eq. (34), and introducing the canonically normalized inflaton

$$\sigma = \sqrt{2K_{SS^*}} |S| \text{ with } K_{SS^*} = 1, \quad (36)$$

the inflationary potential V_I can be cast in the form

$$V_I \simeq V_{I0} (1 + C_{RC} + C_{SSB} + C_{SUGRA}), \quad (37)$$

where the individual contributions are specified as follows:

a. C_{RC} represents the RCs to V_I/V_{I0} which may be written consistently with Eq. (34) as [2]

$$C_{\text{RC}} = \frac{\kappa^2 N_G}{128\pi^2} \left(8 \ln \frac{\kappa^2 M^2}{Q^2} + f_{\text{RC}}(x) \right), \quad (38a)$$

with $x = (\sigma - \sqrt{2}\lambda\langle Z \rangle_1^\nu m_P^{1-\nu}/\kappa)/M > \sqrt{2}$ and

$$f_{\text{RC}}(x) = 8x^2 \tanh^{-1}(2/x^2) - 4(\ln 4 + x^4 \ln x) + (4 + x^4) \ln(x^4 - 4). \quad (38b)$$

b. C_{SSB} is the contribution to V_I/V_{I0} from the soft SUSY-breaking effects [12] parameterized as follows:

$$C_{\text{SSB}} = m_{3/2}^2 \sigma^2 / 2V_{I0} - a_S \sigma / \sqrt{2V_{I0}}, \quad (38c)$$

where the tadpole parameter reads

$$a_S = 2^{1-\nu/2} m \frac{\langle z \rangle_1^\nu}{m_P^\nu} \left(1 + \frac{\langle z \rangle_1^2}{2N m_P^2} \right) \left(2 - \nu - \frac{3\langle z \rangle_1^2}{8\nu m_P^2} \right). \quad (38d)$$

The minus sign results from the minimization of the factor $(S + S^*) = \sqrt{2}\sigma \cos(\theta_S/m_P)$ which occurs for $\theta_S/m_P = \pi \pmod{2\pi}$ – the decomposition of S is shown in Eq. (17). We further assume that θ_S remains constant during FHI. Otherwise, FHI may be analyzed as a two-field model of inflation in the complex plane [15]. Trajectories, though, far from the real axis require a significant amount of tuning. The first term in Eq. (38c) does not play any essential role in our set-up due to low enough $m_{3/2}$'s – cf. Ref. [14].

c. C_{SUGRA} is the SUGRA correction to V_I/V_{I0} , after subtracting the one in C_{SSB} . It reads

$$C_{\text{SUGRA}} = c_{2\nu} \frac{\sigma^2}{2m_P^2} + c_{4\nu} \frac{\sigma^4}{4m_P^4}, \quad (38e)$$

where the relevant coefficients originate from Eqs. (32b) and (32d) and read

$$c_{2\nu} = \langle z \rangle_1^2 / 2m_P^2 \quad \text{and} \quad c_{4\nu} = (1 + \langle z \rangle_1^2 / m_P^2) / 2. \quad (38f)$$

Note that in similar models – cf. Ref. [14, 15] – without the presence of a HS, $c_{2\nu}$ is taken identically equal to zero. Our present set-up shows that this assumption may be well motivated.

III. GENERATION OF THE μ TERM OF MSSM

An important issue, usually related to the inflationary dynamics – see, e.g., Refs. [5, 22, 57] – is the generation of the μ term of MSSM. Indeed, we would like to avoid the introduction by hand into the superpotential of MSSM of a term $\mu H_u H_d$ with μ being an energy scale much lower than the GUT scale – H_u and H_d are the Higgs superfields coupled to the up and down quarks respectively. To avoid this we assign R charges equal to 2 to both H_u and H_d whereas all the other fields of MSSM have zero R charges. Although we employ here the notation used in a \mathbb{G}_{B-L} model, our construction can

be easily extended to the cases of the two other \mathbb{G} 's considered – see Sec. II A 1. Indeed, H_u and H_d are included in a bidoublet superfield belonging to the representation $(1, 2, 2, 0)$ in the case of \mathbb{G}_{LR} [5]. On the other hand, these superfields are included in the representations $(\bar{5}, 2)$ and $(5, -2)$ in the case of \mathbb{G}_{5X} [6].

The mixing term between H_u and H_d may emerge if we incorporate (somehow) into the Kähler potential of our model the following higher order terms

$$K_\mu = \lambda_\mu \frac{Z^{*2\nu}}{m_P^{2\nu}} H_u H_d + \text{h.c.}, \quad (39)$$

where the dimensionless constant λ_μ is taken real for simplicity. To exemplify our approach – cf. Ref. [28] – we complement the Kähler potential in Eq. (5) with terms involving the left-handed chiral superfields of MSSM denoted by Y_α with $\alpha = 1, \dots, 7$, i.e.,

$$Y_\alpha = Q, L, d^c, u^c, e^c, H_d, \quad \text{and} \quad H_u,$$

where the generation indices are suppressed. Namely we consider the following variants of the total K ,

$$K_1 = K_H + K_I + K_\mu + |Y_\alpha|^2, \quad (40a)$$

$$K_2 = N m_P^2 \ln \left(1 + \frac{1}{N} \left(\frac{|Z|^2 - k^2 Z_-^4 / m_P^2}{m_P^2} + K_\mu \right) \right) + K_I + |Y_\alpha|^2, \quad (40b)$$

$$K_3 = N m_P^2 \ln \left(\frac{1 + |Z|^2 - k^2 Z_-^4 / m_P^2 + |Y_\alpha|^2}{N m_P^2} \right) + K_I + K_\mu, \quad (40c)$$

$$K_4 = N m_P^2 \ln \left(1 + \frac{1}{N} \frac{|Z|^2 - k^2 Z_-^4 / m_P^2 + |Y_\alpha|^2}{N m_P^2} + \frac{K_\mu}{N} \right) + K_I. \quad (40d)$$

Expanding these K 's for low values of $S, \Phi, \bar{\Phi}$, and Y_α , we can bring them into the form

$$K \simeq K_H(Z) + K_I + \tilde{K}(Z) \sum_\alpha |Y_\alpha|^2 + \lambda_\mu \left(c_H \frac{Z^{*2\nu}}{m_P^{2\nu}} H_u H_d + \text{h.c.} \right), \quad (41)$$

where \tilde{K} is determined as follows

$$\tilde{K} = \begin{cases} 1 & \text{for } K = K_1, K_4, \\ \left(1 + \frac{|Z|^2 - k^2 Z_-^4 / m_P^2}{m_P^2 N} \right)^{-1} & \text{for } K = K_2, K_3, \end{cases} \quad (42)$$

whereas c_H is found to be

$$c_H = \begin{cases} 1 & \text{for } K = K_1, K_3, \\ \left(1 + \frac{|Z|^2 - k^2 Z_-^4 / m_P^2}{m_P^2 N} \right)^{-1} & \text{for } K = K_2, K_4. \end{cases} \quad (43)$$

Consistently with our hypothesis about the enhanced symmetry of K in Sec. II A 3, we do not consider the possibility of

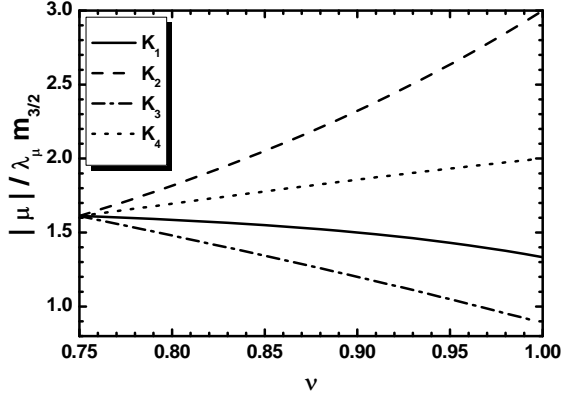


FIG. 3: The ratios $|\mu|/\lambda_\mu m_{3/2}$ for $K = K_1, K_2, K_3$, and K_4 (solid, dashed, dot-dashed, and dotted line respectively) versus ν in the range $0.75 - 1$.

including K_I in the argument of the logarithm of K_H as we have done for K_μ and/or $|Y_\alpha|$.

Applying the relevant formulas of Refs. [28, 37], we find a non-vanishing μ term in the superpotential of MSSM

$$\mu \hat{H}_u \hat{H}_d, \quad (44)$$

where $\hat{Y}_\alpha = \langle \tilde{K} \rangle^{1/2} Y_\alpha$ and the μ parameter reads

$$\frac{|\mu|}{m_{3/2}} = \lambda_\mu \left(\frac{4\nu^2}{3} \right)^\nu \times \begin{cases} (5 - 4\nu) & \text{for } K = K_1, \\ 3(4\nu - 1)/4\nu & \text{for } K = K_2, \\ (5 - 4\nu)\omega & \text{for } K = K_3, \\ 3\omega(4\nu - 1)/4\nu & \text{for } K = K_4. \end{cases} \quad (45)$$

Moreover, in the effective low energy potential we obtain a common soft-SUSY-breaking mass parameter \tilde{m} which is

$$\tilde{m} = m_{3/2} \times \begin{cases} 1 & \text{for } K = K_1 \text{ and } K_2, \\ (3/2\nu - 1) & \text{for } K = K_3 \text{ and } K_4, \end{cases} \quad (46)$$

Therefore, \tilde{m} is a degenerate SUSY mass scale which can indicatively represent the mass level of the SUSY partners. The results in Eqs. (45) and (46) are consistent with those presented in Ref. [28], where further details of the computation are given.

The magnitude of the μ 's in Eq. (45) is demonstrated in Fig. 3, where we present the ratios $|\mu|/\lambda_\mu m_{3/2}$ for $K = K_1$ (solid line), K_2 (dashed line), K_3 (dot-dashed line), and K_4 (dotted line) versus ν for $3/4 < \nu < 1$. By coincidence all cases converge at the value $|\mu|/\lambda_\mu m_{3/2} \simeq 1.6$ for $\nu = 3/4$. For λ_μ 's of order unity, the $|\mu|$ values are a little enhanced w.r.t. $m_{3/2}$ and increase for $K = K_2$ and K_4 or decrease for $K = K_1$ and K_3 as ν increases.

IV. REHEATING STAGE

Soon after FHI the Hubble rate H becomes of the order of their masses and the IS and z enter into an oscillatory

phase about their minima and eventually decay via their coupling to lighter degrees of freedom. Note that θ remains well stabilized at zero during and after FHI and so it does not participate in the phase of damped oscillations. Since $\langle z \rangle \sim m_P$ – see Eq. (22) –, the initial energy density of its oscillations is $\rho_{zI} \sim m_z^2 \langle z \rangle^2$. It is comparable with the energy density of the universe at the onset of these oscillations $\rho_t = 3m_P^2 H^2 \simeq 3m_P^2 m_z^2$ and so we expect that z will dominate the energy density of the universe until completing its decay through its weak gravitational interactions. Actually, this is a representative case of the infamous cosmic moduli problem [38, 39] where reheating is induced by long-lived massive particles with mass around the weak scale.

The reheating temperature is determined by [58]

$$T_{\text{rh}} = (72/5\pi^2 g_{\text{rh}*})^{1/4} \Gamma_{\delta z}^{1/2} m_P^{1/2}, \quad (47)$$

where $g_{\text{rh}*} \simeq 10.75 - 100$ counts the effective number of the relativistic degrees of freedom at T_{rh} . Moreover, the total decay width $\Gamma_{\delta z}$ of the (canonically normalized) sgoldstino

$$\hat{\delta z} = \langle K_{ZZ^*}^{1/2} \rangle \delta z \quad \text{with } \delta z = z - \langle z \rangle \quad \text{and } \langle K_{ZZ^*} \rangle = \langle \omega \rangle^{-2} \quad (48)$$

predominantly includes the contributions from its decay into pseudo-sgoldstinos and higgs via the kinetic terms $K_{ZZ^*} \partial_\mu Z \partial^\mu Z^*$ [39–42] of the Lagrangian. In particular, we have

$$\Gamma_{\delta z} \simeq \Gamma_\theta + \Gamma_{\tilde{h}}, \quad (49)$$

where the individual decay widths are given by

$$\Gamma_\theta \simeq \frac{\lambda_\theta^2 m_z^3}{32\pi m_P^2} \sqrt{1 - 4m_\theta^2/m_{3/2}^2} \quad (50a)$$

with $\lambda_\theta = -\langle z \rangle / N m_P = (4\nu - 3)/\sqrt{6}\nu$, and

$$\Gamma_{\tilde{h}} = \frac{3^{2\nu+1}}{2^{4\nu+1}} \lambda_\mu^2 \frac{\omega^2}{4\pi} \frac{m_z^3}{m_P^2} \nu^{-4\nu}. \quad (50b)$$

Other possible decay channels into gauge bosons through anomalies and three-body MSSM (s)particles are subdominant. On the other hand, we kinematically block the decay of $\hat{\delta z}$ into \tilde{G} 's [39, 44] in order to protect our setting from complications with BBN due to possible late decay of the produced \tilde{G} and problems with the abundance of the subsequently produced lightest SUSY particles. In view of Eqs. (25c) and (25a), this aim can be elegantly achieved if we set $\nu > 3/4$.

Taking κ and m_z values allowed by the inflationary part of our model – see Sec. VI – and selecting some specific K from Eqs. (40a) – (40d), we evaluate T_{rh} as a function of κ and determine the regions allowed by the BBN constraints in Eqs. (59a) and (59b) – see Sec. V below. The results of this computation are displayed in Fig. 4, where we design allowed contours in the $\kappa - T_{\text{rh}}$ plane for the various N_G 's and $\nu = 7/8$. This is an intermediate value in the selected margin $(3/4 - 1)$. The boundary curves of the allowed regions correspond to $\mu = \tilde{m}$ or $\lambda_\mu = 0.65$ (dot-dashed line) and

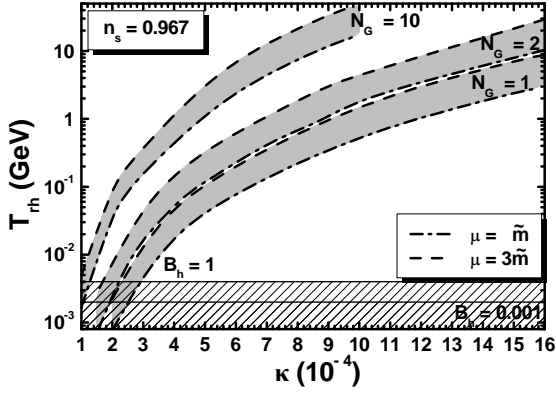


FIG. 4: Allowed strips in the $\kappa - T_{\text{rh}}$ plane compatible with the inflationary requirements in Sec. V for $n_s = 0.967$, and various N_G values indicated in the graph. We take $K = K_1$, $\nu = 7/8$, and $\mu = \tilde{m}$ (dot-dashed lines) or $\mu = 3\tilde{m}$ (dashed lines). The BBN lower bounds on T_{rh} for hadronic branching ratios $B_h = 1$ and 0.001 are also depicted by two thin lines.

$\mu = 3\tilde{m}$ or $\lambda_\mu = 1.96$ (dashed line). The $|\mu|/\tilde{m} - \lambda_\mu$ correspondence is determined via Eq. (45) for a selected K . Here we set $K = K_1$. Qualitatively similar results are obtained for an alternative K choice. We see that there is an ample parameter space consistent with the BBN bounds depicted by two horizontal lines. Since the satisfaction of the inflationary requirements leads to an increase of the scale m with N_G and m heavily influences m_z and consequently T_{rh} – see Eq. (47) – this temperature increases with N_G . The maximal values of T_{rh} for the selected ν are obtained for $\mu = 3\tilde{m}$ and are estimated to be

$$T_{\text{rh}}^{\text{max}} \simeq 14 \text{ GeV}, 33 \text{ GeV}, \text{ and } 49 \text{ GeV} \quad (51)$$

for $N_G = 1, 2$, and 10 respectively. Obviously, reducing μ below \tilde{m} , the parameters λ_μ , $\Gamma_{\delta z}$, and so T_{rh} decrease too and the slice cut by the BBN bound increases. Therefore, our setting fits better with high-scale SUSY [53] and not with split [53] or natural [39] SUSY which assume $\mu \ll \tilde{m}$.

V. OBSERVATIONAL REQUIREMENTS

Our set-up must satisfy a number of observational requirements specified below.

a. The number of e-foldings that the pivot scale k_* = $0.05/\text{Mpc}$ undergoes during FHI must be adequately large for the resolution of the horizon and flatness problems of standard Big Bang cosmology. Assuming that FHI is followed, in turn, by a decaying-particle, radiation and matter dominated era, we can derive the relevant condition [7, 18]:

$$N_{I*} = \int_{\sigma_f}^{\sigma_*} \frac{d\sigma}{m_P^2} \frac{V_I}{V_I'} \simeq 19.4 + \frac{2}{3} \ln \frac{V_{I0}^{1/4}}{1 \text{ GeV}} + \frac{1}{3} \ln \frac{T_{\text{rh}}}{1 \text{ GeV}}, \quad (52)$$

where the prime denotes derivation w.r.t. σ , σ_* is the value of σ when k_* crosses outside the inflationary horizon, and σ_f is the value of σ at the end of FHI. The latter coincides with either the critical point $\sigma_c = \sqrt{2}|S_c|$ – see Eq. (33) –, or the value of σ for which one of the slow-roll parameters [1]

$$\epsilon = m_P^2 \left(V_I' / \sqrt{2} V_I \right)^2 \quad \text{and} \quad \eta = m_P^2 V_I'' / V_I \quad (53)$$

exceeds unity in absolute value. For $\lambda \sim 10^{-12}$ as required by the cosmic coincidence problem – see below – we obtain $\langle \sigma \rangle \simeq 0$ which does not disturb the inflationary dynamics since $\langle \sigma \rangle \ll \sigma_c$.

b. The amplitude A_s of the power spectrum of the curvature perturbation generated by σ during FHI and calculated at k_* as a function of σ_* must be consistent with the data [19], i.e.,

$$\sqrt{A_s} = \frac{1}{2\sqrt{3}\pi m_P^3} \frac{V_I^{3/2}(\sigma_*)}{|V_I'(\sigma_*)|} \simeq 4.588 \times 10^{-5}. \quad (54)$$

The observed curvature perturbation is generated wholly by σ since the other scalars are adequately massive during FHI – see Sec. II C 1.

c. The scalar spectral index n_s , its running α_s , and the scalar-to-tensor ratio r must be in agreement with the fitting of the *Planck* TT, TE, EE+lowE+lensing, *BICEP/Keck Array* (BK18), and BAO data [7, 20] with the $\Lambda\text{CDM}+r$ model which approximately requires that, at 95% confidence level (c.l.),

$$n_s = 0.967 \pm 0.0074 \quad \text{and} \quad r \leq 0.032, \quad (55)$$

with $|\alpha_s| \ll 0.01$. These observables are calculated employing the standard formulas

$$n_s = 1 - 6\epsilon_* + 2\eta_*, \quad (56a)$$

$$\alpha_s = 2(4\eta_*^2 - (n_s - 1)^2)/3 - 2\xi_*, \quad \text{and} \quad r = 16\epsilon_*, \quad (56b)$$

where $\xi \simeq m_P^4 V_I' V_I''' / V_I^2$ and all the variables with the subscript $*$ are evaluated at $\sigma = \sigma_*$.

d. The dimensionless tension $G\mu_{\text{cs}}$ of the $B - L$ CSs produced at the end of FHI in the case $\mathbb{G} = \mathbb{G}_{B-L}$ is [59]

$$G\mu_{\text{cs}} \simeq \frac{1}{2} \left(\frac{M}{m_P} \right)^2 \epsilon_{\text{cs}}(r_{\text{cs}}) \quad \text{with} \quad \epsilon_{\text{cs}}(r_{\text{cs}}) = \frac{2.4}{\ln(2/r_{\text{cs}})}. \quad (57)$$

Here $G = 1/8\pi m_P^2$ is the Newton gravitational constant and $r_{\text{cs}} = \kappa^2/2g^2 \leq 10^{-2}$ with $g \simeq 0.7$ being the gauge coupling constant at a scale close to M . $G\mu_{\text{cs}}$ is restricted by the level of the CS contribution to the observed anisotropies of CMB radiation reported by *Planck* [29] as follows:

$$G\mu_{\text{cs}} \lesssim 2.4 \times 10^{-7} \quad \text{at } 95\% \text{ c.l.} \quad (58a)$$

On the other hand, the primordial CS loops and segments connecting monopole pairs decay by emitting stochastic gravitational radiation which is measured by the pulsar timing array experiments [32, 33]. If the CS network is stable, the recent observations require [31]

$$G\mu_{\text{cs}} \lesssim 2 \times 10^{-10} \quad \text{at } 95\% \text{ c.l.} \quad (58b)$$

However, if the CSs are metastable, due to the embedding of \mathbb{G}_{B-L} into a larger group \mathbb{G}_{GUT} whose breaking leads to monopoles which can break the CSs, the interpretation [31] of the recent observations [32, 33] dictates

$$10^{-8} \lesssim G\mu_{\text{cs}} \lesssim 2 \times 10^{-7} \text{ for } 8.2 \gtrsim \sqrt{r_{\text{ms}}} \gtrsim 7.9 \quad (58\text{c})$$

at 2σ where the upper bound originates from Ref. [34] and is valid for a standard cosmological evolution and CSs produced after inflation. Here r_{ms} is the ratio of the monopole mass squared to μ_{cs} . Since we do not specify further this possibility in our work, the last restriction does not impact on our parameters.

e. Consistency between theoretical and observational values of light element abundances predicted by BBN imposes a lower bound on T_{rh} , which depends on the mass of the decaying particle z and the hadronic branching ratio B_{h} . Namely, for large $m_z \sim 10^5$ GeV, the most up-to-date analysis of Ref. [43] entails

$$T_{\text{rh}} \geq 4.1 \text{ MeV for } B_{\text{h}} = 1 \quad (59\text{a})$$

$$\text{and } T_{\text{rh}} \geq 2.1 \text{ MeV for } B_{\text{h}} = 10^{-3}. \quad (59\text{b})$$

The BBN bound is mildly softened for larger m_z values. Moreover, the possible production of \tilde{G} from the z decay is mostly problematic [39] since it may lead to overproduction of the LSP (i.e., the lightest SUSY particle), whose non-thermally produced abundance from the \tilde{G} decay can drastically overshadow its thermally-produced one. As a consequence, the LSP abundance can easily violate the observational upper bound [19] from CDM considerations. This is the moduli-induced [44] LSP overproduction problem via the \tilde{G} decay [39]. To avoid this complication, we kinematically forbid the decay of z into \tilde{G} selecting $\nu > 3/4$ which ensures that $m_z < 2m_{3/2}$ – see Eq. (25c).

f. We identify $\langle V_{\text{F}} \rangle$ in Eq. (23) with the DE energy density, i.e.,

$$\langle V_{\text{F}} \rangle = \Omega_{\Lambda} \rho_{\text{c}0} = 7.2 \times 10^{-121} m_{\text{P}}^4, \quad (60)$$

where $\Omega_{\Lambda} = 0.6889$ and $\rho_{\text{c}0} = 2.4 \times 10^{-120} h^2 m_{\text{P}}^4$ with $h = 0.6732$ [19] are the density parameter of DE and the current critical energy density of the universe respectively. By virtue of Eq. (23), we see that Eq. (60) can be satisfied for $\lambda \sim m/m_{\text{P}}$. Explicit values are given for the cases in Table I.

g. Scenarios with large \tilde{m} , although not directly accessible at the LHC, can be probed via the measured value of the Higgs boson mass. Within high-scale SUSY, updated analysis requires [52, 53]

$$3 \times 10^3 \lesssim \tilde{m}/\text{GeV} \lesssim 3 \times 10^{11}, \quad (61)$$

for degenerate sparticle spectrum, μ and $\tan\beta$ in the ranges $\tilde{m}/3 \lesssim \mu \leq 3\tilde{m}$ and $1 \leq \tan\beta \leq 50$, and varying the stop mixing.

VI. RESULTS

As induced from Secs. II A 1 – II A 3 and III, our model depends on the parameters

$$N_{\text{G}}, \kappa, M, m, \lambda, \nu, k, \text{ and } \lambda_{\mu}$$

(recall that N is related to ν via Eq. (7)). Let us initially clarify that λ can be fixed at a rather low value as explained below Eq. (60) and does not influence the rest of our results. Moreover, k affects m_{θ} and $m_{1\theta}$ via Eqs. (25c) and (31a) and helps us to avoid massless modes. We take $k = 0.1$ throughout our investigation.

As shown in Ref. [14], the confrontation of FHI with data for any fixed N_{G} requires a specific adjustment between κ or M and the a_{S} which is given in Eq. (38d) as a function of m , ν , κ , and M – see Eq. (30). Obviously a specific a_{S} value can be obtained by several choices of the initial parameters ν and m . These parameters influence also the requirement in Eq. (52) via T_{rh} , which is given in Eq. (47). However, to avoid redundant solutions we first explore our results for the IS in terms of the variables κ, M , and a_{S} in Sec. VI A taking a representative T_{rh} value, e.g., $T_{\text{rh}} \simeq 1$ GeV. Variation of T_{rh} over one or two orders of magnitude does not affect our findings in any essential way. Therefore, we do not impose in Sec. VI A the constraints from the BBN in Eqs. (59a) and (59b). In Sec. VI B, we then interconnect these results with the HS parameters ν and m .

A. Inflation Analysis

Enforcing the constraints in Eqs. (52) and (54) we can find M and σ_{\star} , for any given N_{G} , as functions of our free parameters κ and a_{S} . Let us clarify here that for $N_{\text{G}} = 1$ the parameter space is identical with the one explored in Ref. [14], where the HS is not specified. As explained there – see also Ref. [15] – observationally acceptable values of n_{s} can be achieved by implementing hilltop FHI. This type of FHI requires a non-monotonic V_{I} with σ rolling from its value σ_{max} at which the maximum of V_{I} lies down to smaller values. As for any model of hilltop inflation, V_{I}' and therefore ϵ in Eq. (53) and r in Eq. (56b) decrease sharply as $N_{\text{I}\star}$ increases – see Eq. (52) –, whereas V_{I}'' (or η) becomes adequately negative, thereby lowering n_{s} within its range in Eq. (55).

These qualitative features are verified by the approximate computation of the quantities in Eq. (53) for $\sigma < \sigma_{\text{max}}$ which are found to be

$$\epsilon \simeq m_{\text{P}}^2 (C'_{\text{RC}} + C'_{\text{SSB}})^2 / 2 \text{ and } \eta \simeq m_{\text{P}}^2 C''_{\text{RC}}, \quad (62)$$

where the derivatives of the various contributions read

$$C'_{\text{SSB}} \simeq -a_{\text{S}} / \sqrt{2V_{\text{I}0}}, \quad (63\text{a})$$

$$C'_{\text{RC}} \simeq \frac{N_{\text{G}} \kappa^2 x}{32M\pi^2} (4 \tanh^{-1}(2/x^2) + x^2 \ln(1 - 4/x^4)), \quad (63\text{b})$$

$$C''_{\text{RC}} \simeq \frac{N_{\text{G}} \kappa^2}{32M^2\pi^2} (4 \tanh^{-1}(2/x^2) + 3x^2 \ln(1 - 4/x^4)). \quad (63\text{c})$$

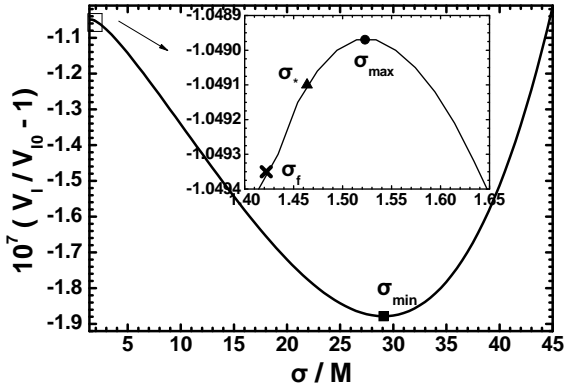


FIG. 5: V_I as a function of σ in units of M for the parameters given in column B of Table I. The values σ_* , σ_f , σ_{\max} , and σ_{\min} of σ are also depicted.

The required behavior of V_I in Eq. (37) can be attained, for given N_G , thanks to the similar magnitudes and the opposite signs of the terms C'_{RC} and C'_{SSB} in Eqs. (63a) and (63b) which we can obtain for carefully selecting κ and a_S . Apparently, we have $C'_{SSB} < 0$ and $C'_{RC} > 0$ for $\sigma_* < \sigma_{\max}$ since $|4 \tanh^{-1}(2/x^2)| > |x^2 \ln(1 - 4/x^4)|$. On the contrary, $C'_{RC} < 0$, since the negative contribution $3x^2 \ln(1 - 4/x^4)$ dominates over the first positive one, and so we obtain $\eta < 0$ giving rise to acceptably low n_s values.

We can roughly determine σ_{\max} by expanding C'_{RC} for large σ and equating the result with C'_{SSB} . We obtain

$$\frac{N_G \kappa^2}{8\pi^2 \sigma_{\max}} = \frac{a_S}{\sqrt{2} \kappa M^2} \Rightarrow \sigma_{\max} \simeq \frac{\kappa^3 M^2 N_G}{4\sqrt{2} \pi^2 a_S}. \quad (64)$$

Needless to say, V_I turns out to be bounded from below for large σ 's since in this regime C_{SUGRA} starts dominating over C_{RC} generating thereby a (N_G -independent) minimum at about

$$\sigma_{\min} \simeq \left(\frac{a_S m_P^4}{\sqrt{2} c_{4\nu} \kappa M^2} \right)^{1/3}. \quad (65)$$

For $\sigma > \sigma_{\min}$, V_I becomes a monotonically increasing function of σ and so the boundedness of V_I is assured.

From our numerical computation we observe that, for constant N_G , κ , and a_S , the lower the value for n_s we wish to attain, the closer we must set σ_* to σ_{\max} . Given that σ_{\max} turns out to be comparable to σ_c and the hierarchy $\sigma_c < \sigma_* < \sigma_{\max}$ has to hold, we see that we need two types of mild tunings in order to obtain successful FHI. To quantify the amount of these tunings, we define the quantities

$$\Delta_{c*} = \frac{\sigma_* - \sigma_c}{\sigma_c} \quad \text{and} \quad \Delta_{\max*} = \frac{\sigma_{\max} - \sigma_*}{\sigma_{\max}}. \quad (66)$$

The naturalness of the hilltop FHI increases with Δ_{c*} and $\Delta_{\max*}$. To get an impression of the amount of these tunings and their dependence on the parameters of the model, we display in Table I the resulting Δ_{c*} and $\Delta_{\max*}$ together with M ,

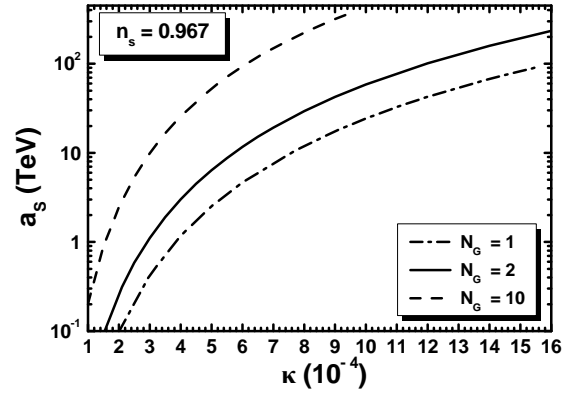


FIG. 6: Values of a_S allowed by Eqs. (52) and (54) versus κ for various N_G 's and fixed $n_s = 0.967$.

a_S , α_s , and r for $\kappa = 0.0005$ and n_s fixed to its central value in Eq. (55). In all cases, we obtain $N_{I*} \simeq 40.5$ from Eq. (52). We notice that $\Delta_{\max*} > \Delta_{c*}$ and that their values may be up to 10% increasing with N_G (and a_S). Recall that in Ref. [14] it is shown that Δ_{c*} and $\Delta_{\max*}$ increase with κ (and M). From the observables listed in Table I we also infer that $|\alpha_s|$ turns out to be of order 10^{-4} , whereas r is extremely tiny, of order 10^{-11} , and therefore far outside the reach of the forthcoming experiments devoted to detect primordial gravity waves. For the preferred n_s values, we observe that r and $|\alpha_s|$ increase with a_S .

The structure of V_I described above is visualized in Fig. 5, where we display a typical variation of V_I as a function of σ/M for the values of the parameters shown in column B of Table I. The maximum of V_I is located at $\sigma_{\max}/M = 1.52 \{1.38\}$, whereas its minimum lies at $\sigma_{\min}/M = 29.1 \{29.5\}$ – the values obtained via the approximate Eqs. (64) and (65) are indicated in curly brackets. The values of $\sigma_*/M \simeq 1.4637$ and $\sigma_f/M \simeq 1.41421$ are also depicted together with σ_{\max}/M in the subplot of this figure. We remark that the key σ values for the realization of FHI are squeezed very close to one another and so their accurate determination is essential for obtaining reliable predictions from Eqs. (56a) and (56b). Moreover, N_{I*} in Eq. (52) can only be found numerically taking all the possible contributions to V_I' from Eqs. (63a) and (63b) and thus σ_* can not be expressed analytically in terms of N_{I*} . For these reasons, the results presented in the following are exclusively based on our numerical analysis.

We first display in Fig. 6 the contours which are allowed by Eqs. (52) and (54) in the $\kappa - a_S$ plane taking $n_s = 0.967$ and $N_G = 1$ (dot-dashed line), $N_G = 2$ (solid line), and $N_G = 10$ (dashed line). The various lines terminate at κ values close to 10^{-3} beyond which no observationally acceptable inflationary solutions are possible. We do not depict the very narrow strip obtained for each N_G by varying n_s in its allowed range in Eq. (55), since the obtained boundaries are almost indistinguishable. From the plotted curves we notice that the required a_S 's increase with N_G .

Working in the same direction, we delineate in Fig. 7 the

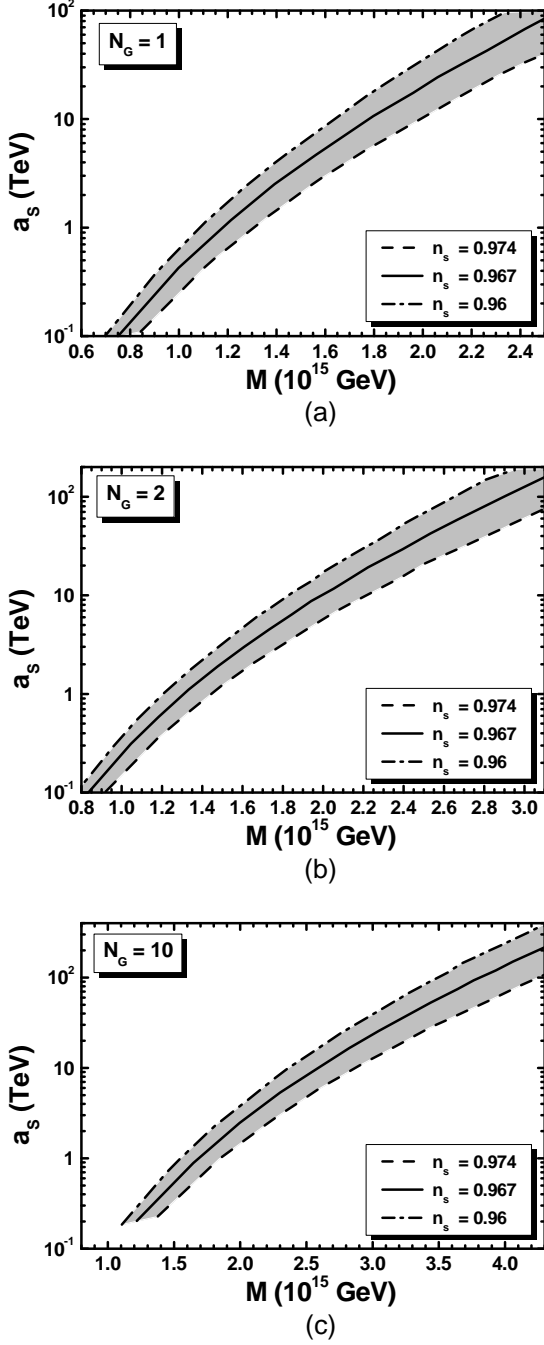


FIG. 7: Regions (shaded) allowed by Eqs. (52), (54), and (55) in the $M - a_s$ plane for various N_G 's. The conventions adopted for the various lines are also shown.

regions in the $M - a_s$ plane allowed by Eqs. (52), (54), and (55) for the considered \mathbb{G} 's. In particular, we use $N_G = 1, 2$, and 10 in subfigures (a), (b), and (c) respectively. The boundaries of the allowed areas in Fig. 7 are determined by the dashed [dot-dashed] lines corresponding to the upper [lower] bound on n_s in Eq. (55). We also display by solid lines the allowed contours for $n_s = 0.967$. We observe that the maximal allowed M 's increase with N_G . The maximal r 's are en-

countered in the upper right end of the dashed lines, which correspond to $n_s = 0.974$, with the maximal value being $r = 6.2 \times 10^{-10}$ for $N_G = 10$. On the other hand, the maximal $|\alpha_s|$'s are achieved along the dot-dashed lines and the minimal value of α_s is -3.2×10^{-4} for $N_G = 10$ too. Summarizing our findings from Fig. 7 for the central n_s value in Eq. (55) and $N_G = 1, 2$, and 10 respectively we end up with the following ranges:

$$0.07 \lesssim M/10^{15} \text{ GeV} \lesssim 2.56 \text{ and } 0.1 \lesssim a_s/\text{TeV} \lesssim 100, \quad (67a)$$

$$0.82 \lesssim M/10^{15} \text{ GeV} \lesssim 3.7 \text{ and } 0.09 \lesssim a_s/\text{TeV} \lesssim 234, \quad (67b)$$

$$1.22 \lesssim M/10^{15} \text{ GeV} \lesssim 4.77 \text{ and } 0.2 \lesssim a_s/\text{TeV} \lesssim 460. \quad (67c)$$

Within these margins, Δ_{c*} ranges between 0.5% and 20% and $\Delta_{\max*}$ between 0.4% and 12%. The lower bounds of these inequalities are expected to be displaced to slightly larger values due to the post-inflationary requirements in Eqs. (59a) and (59b) which are not considered here for the shake of generality. Recall that precise incorporation of these constraints requires the adoption of a specific K from Eqs. (40a) – (40d) and corresponding μ/\tilde{m} relation from Eq. (45).

In the case $\mathbb{G} = \mathbb{G}_{B-L}$, CSs may be produced after FHI with $G\mu_{cs} = (6.5-89) \times 10^{-9}$ for the parameters in Eq. (67a). Therefore, the corresponding parameter space is totally allowed by Eq. (58a) but completely excluded by Eq. (58b), if the CSs are stable. If these CSs are metastable, the explanation [30] of the recent data [32, 33] on stochastic gravity waves is possible for $M \gtrsim 9 \times 10^{14} \text{ GeV}$ in Eq. (67a) where Eq. (58c) is fulfilled. No similar restrictions exist if $\mathbb{G} = \mathbb{G}_{LR}$ or \mathbb{G}_{5X} , which do not lead to the production of any cosmic defect. On the other hand, the unification of gauge coupling constants within MSSM close to $M_{\text{GUT}} = 2.86 \times 10^{16} \text{ GeV}$ remains intact if $\mathbb{G} = \mathbb{G}_{B-L}$ despite the fact that $M \ll M_{\text{GUT}}$ for M given in Eq. (67a). Indeed, the gauge boson associated with the $U(1)_{B-L}$ breaking is neutral under \mathbb{G}_{SM} and so it does not contribute to the relevant renormalization group running. If $\mathbb{G} = \mathbb{G}_{LR}$ or \mathbb{G}_{5X} we may invoke threshold corrections or additional matter supermultiples to restore the gauge coupling unification – for $\mathbb{G} = \mathbb{G}_{5X}$ see Ref. [60].

B. Link to the MSSM

The inclusion of the HS in our numerical computation assists us to gain information about the mass scale of the SUSY particles through the determination of $\tilde{m} \sim m_{3/2}$ – see Eq. (46). Indeed, a_s , which is already restricted as a function of κ or M for given N_G in Figs. 6 and 7, can be correlated to m via Eq. (38d). Taking into account Eq. (30) and the fact that $\langle z \rangle_I/m_P \sim 10^{-3}$ – see Table I – we can solve analytically and very accurately Eq. (38d) w.r.t. m . We find

$$m \simeq \left(\frac{a_s}{2^{1+\nu}(2-\nu)} \right)^{(2-\nu)/2} \left(\frac{3H_I^2}{(1-\nu)\nu^2} \right)^{\nu/4}. \quad (68)$$

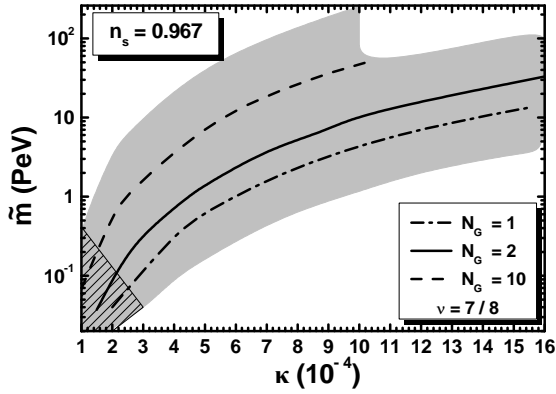


FIG. 8: Region in the $\kappa - \tilde{m}$ plane allowed by Eqs. (52) and (54) for $K = K_1$, $\mu = \tilde{m}$, $n_s = 0.967$, and $1 \leq N_G \leq 10$, $3/4 < \nu < 1$. The allowed contours for $\nu = 7/8$ are also depicted. Hatched is the region excluded by BBN for $B_h = 0.001$.

Let us clarify here that in our numerical computation we use an iterative process, which though converges quickly, in order to extract consistently m as a function of κ and M . This is because the determination of the latter parameters via the conditions in Eqs. (52) and (54) requires the introduction of a trial m value which allows us to use as input the form of V_I in Eq. (37). Thanks to the aforementioned smallness of $\langle z \rangle_I$ in Eq. (38d), m turns out to be two to three orders of magnitude larger than a_S , suggesting that \tilde{m} lies clearly at the PeV scale via Eqs. (46) and (25a). In fact, taking advantage of the resulting m for fixed ν in Eq. (68), we can compute $m_{3/2}$ from Eq. (25a), and m_z and m_θ from Eq. (25c). All these masses turn out to be of the same order of magnitude – see Table I. Then \tilde{m} and T_{rh} can be also estimated from Eqs. (46) and (47) for a specific K from Eqs. (40a) – (40d). The magnitude of \tilde{m} and the necessity for $\mu \sim \tilde{m}$, established in Sec. IV, hints towards the high-scale MSSM.

To highlight numerically our expectations, we take $K = K_1$ and fix initially $\nu = 7/8$, which is a representative value. The predicted \tilde{m} as a function of κ is depicted in Fig. 8 for the three N_G 's considered in our work. We use the same type of lines as in Fig. 6. Assuming also that $\mu = \tilde{m}$ we can determine the segments of these lines that can be excluded by the BBN bound in Eq. (59b). In all, we find that \tilde{m} turns out to be confined in the ranges

$$0.34 \lesssim \tilde{m}/\text{PeV} \lesssim 13.6 \text{ for } N_G = 1, \quad (69a)$$

$$0.21 \lesssim \tilde{m}/\text{PeV} \lesssim 32.9 \text{ for } N_G = 2, \quad (69b)$$

$$0.58 \lesssim \tilde{m}/\text{PeV} \lesssim 46.8 \text{ for } N_G = 10. \quad (69c)$$

Allowing ν and μ to vary within their possible respective margins (0.75–1) and $(1-3)\tilde{m}$, we obtain the gray shaded region in Fig. 8. We present an overall region for the three possible N_G 's, since the separate ones overlap each other. Obviously the lower boundary curve of the displayed region is obtained for $N_G = 1$ and $\nu \simeq 0.751$, whereas the upper one corresponds to $N_G = 10$ and $\nu \simeq 0.99$. The hatched region is

ruled out by Eq. (59b). All in all, we obtain the predictions

$$1.2 \lesssim a_S/\text{TeV} \lesssim 460 \text{ and } 0.09 \lesssim \tilde{m}/\text{PeV} \lesssim 253 \quad (70)$$

and $T_{\text{rh}}^{\text{max}} \simeq 71 \text{ GeV}$, 139 GeV , and 163 GeV for $N_G = 1, 2$, and 10 respectively attained for $\mu = 3\tilde{m}$ and $\nu \simeq 0.99$. The derived allowed margin of \tilde{m} , which is included in Eq. (61), and the employed μ values render our proposal compatible with the mass of the Higgs boson discovered in LHC [52] if we adopt as a low energy effective theory the high-scale version of MSSM [53].

VII. CONCLUSIONS

We considered the realization of FHI in the context of an extended model based on the superpotential and Kähler potential in Eqs. (1) and (5), which are consistent with an approximate R symmetry. The minimization of the SUGRA scalar potential at the present vacuum constrains the curvature of the internal space of the goldstino superfield and provides a tunable energy density which may be interpreted as the DE without the need of an unnaturally small coupling constant. On the other hand, this same potential causes a displacement of the sgoldstino to values much smaller than m_P during FHI. Combining this fact with minimal kinetic terms for the inflaton, the η problem is resolved allowing hilltop FHI. The slope of the inflationary path is generated by the RCs and a tadpole term with a minus sign and values which increase with the dimensionality of the representation of the relevant Higgs superfields. Embedding \mathbb{G}_{B-L} into a larger gauge group \mathbb{G}_{GUT} which predicts the production of monopoles prior to FHI that can eventually break the CSs allows the attribution of the observed data on the gravitational waves to the decay of metastable $B-L$ CSs.

We also discussed the generation of the μ term of MSSM following the Giudice-Masiero mechanism and restricted further the curvature of the goldstino internal space so that phenomenologically dangerous production of \tilde{G} may be avoided. This same term assists in the decay of the sgoldstino, which normally dominates the energy density of the universe, at a reheat temperature which can be as high as 163 GeV provided that the μ parameter is of the order of the \tilde{G} mass, i.e., of order PeV. Linking the inflationary sector to a degenerate MSSM mass scale \tilde{m} we found that \tilde{m} lies in a range consistent with the Higgs boson mass measured at LHC within high-scale SUSY.

The long-lasting matter domination obtained in our model because of the sgoldstino oscillations after the end of FHI leads [61] to a suppression at relatively large frequencies ($f > 0.1 \text{ Hz}$) of the spectrum of the gravitational waves from the decay of the metastable CSs. This effect may be beneficial for spectra based on $G\mu_{\text{CS}}$ values which violate the upper bound of Eq. (58c) from the results of Ref. [34]. Since we do not achieve such $G\mu_{\text{CS}}$ values here we do not analyze further this implication of our scenario. On the other hand, the low reheat temperature encountered in our proposal makes difficult the achievement of baryogenesis. However, there are

currently attempts [62] based on the idea of cold electroweak baryogenesis [63] which may overcome this problem. It is also not clear which particle could play the role of CDM in a high-scale SUSY regime. Let us just mention that a thorough investigation is needed including the precise solution of the relevant Boltzmann equations as in Ref. [58] in order to assess if the abundance of the lightest SUSY particle can be confined within the observational limits in this low-reheating scenario.

Acknowledgments

We would like to thank I. Antoniadis, H. Baer, and E. Kiritsis for useful discussions. This research work was supported by the Hellenic Foundation for Research and Innovation (H.F.R.I.) under the “First Call for H.F.R.I. Research Projects to support Faculty members and Researchers and the procurement of high-cost research equipment grant” (Project Number: 2251).

Appendix: SUGRA CORRECTIONS TO THE INFLATIONARY POTENTIAL of FHI

As shown in Sec. II C 2, the presence of W_H and K_H in Eqs. (2b) and (6b) respectively transmit (potentially important) corrections to the inflationary potential. We present here, for the first time to the best of our knowledge, these corrections without specify the form of these functions. The corrections from the IS are also taken into account.

In particular, we consider the following superpotential and Kähler potential resulting from the ones in Eqs. (1) and (5) by setting Φ and $\bar{\Phi}$ to zero:

$$W = W_I(S) + W_H(Z) \text{ and } K = K_I(S) + K_H(Z), \quad (\text{A.1})$$

where W_I and K_I are given by

$$W_I = -\hat{\kappa} M^2 S \text{ and } K_I = K_I(|S|^2) \quad (\text{A.2})$$

(cf. Eqs. (2a) and (6a)). We also assume that K_I can be reliably expanded in powers of $|S|/m_P$ as follows:

$$K_I \simeq |S|^2 + \frac{k_4}{4} \frac{|S|^4}{m_P^2} + \frac{k_6}{9} \frac{|S|^6}{m_P^3} + \dots \quad (\text{A.3})$$

Under these circumstances, the inverse Kähler metric reads

$$K_I^{SS*} \simeq 1 - k_4 |S|^2 m_P^2 + (k_4^2 - k_6) |S|^4 / m_P^4 + \dots \quad (\text{A4a})$$

and the exponential prefactor of V_F in Eq. (9) is well approximated by

$$e^{K_I/m_P^2} \simeq 1 + \frac{|S|^2}{m_P^2} + \frac{1+2k_4}{2} \frac{|S|^4}{m_P^4} + \dots \quad (\text{A4b})$$

Taking into account the two last expressions and expanding V_F in Eq. (9) with W and K from Eq. (A.1) up to the forth power in $|S|/m_P$, we obtain the quite generic formula below

$$V_F \simeq v_0 + m_{I3/2}^2 |S|^2 + (v_1 S^* + \text{c.c.}) + v_2 |S|^2 / m_P^2 + (v_3 S^* + \text{c.c.}) |S|^2 / m_P^2 + v_4 |S|^4 / m_P^4 + \dots, \quad (\text{A.5})$$

where the various v 's are found to be

$$v_0 = \kappa^2 M^4, \quad (\text{A6a})$$

$$v_1 = \kappa M^2 m_{I3/2} \left\langle 2 - K_H^{ZZ*} \partial_Z G_H \right\rangle_I, \quad (\text{A6b})$$

$$v_2 = \kappa^2 M^4 \left\langle K_H^{ZZ*} |\partial_Z K_H|^2 / m_P^2 - k_4 \right\rangle_I, \quad (\text{A6c})$$

$$v_3 = \kappa M^2 m_{I3/2} \left\langle (1 + k_4/2) - K_H^{ZZ*} \partial_Z G_H \right\rangle_I, \quad (\text{A6d})$$

$$v_4 = \kappa^2 M^4 \left(1/2 + k_4(4k_4 - 7)/4 - k_6 + \left\langle K_H^{ZZ*} |\partial_Z K_H|^2 / m_P^2 \right\rangle_I \right). \quad (\text{A6e})$$

Here κ is the rescaled coupling constant $\hat{\kappa}$ after absorbing the relevant prefactor $e^{(K_H)_I/2m_P^2}$ in Eq. (9) and we used the definition of the \tilde{G} mass

$$m_{I3/2} = \left\langle e^{K_H/2m_P^2} W_H / m_P^2 \right\rangle_I,$$

and the Kähler invariant function, see, e.g., Ref. [56],

$$G_H = K_H / m_P^2 + \ln |W_H / m_P^3|^2. \quad (\text{A.7})$$

From these results we see that v_2 and v_4 generically receive contributions from both the IS and HS, whereas v_1 and v_3 exclusively from the HS – cf. Refs. [8, 10]. Specifically, from Eq. (A6c), we can recover the miraculous cancellation occurring within minimal FHI [4, 14], where the HS is ignored and $k_4 = k_6 = 0$ in Eq. (A.3). Switching on K_H and noticing that

$$k_4 = \partial_S^2 \partial_{S^*}^2 K_I(S = S^* = 0), \quad (\text{A.8})$$

we can also see that Eq. (A6c) agrees with that presented in Ref. [8]. The applicability of our results can be easily checked for other HS settings [23, 24, 26] too.

References

-
- [1] J. Martin, C. Ringeval, and V. Vennin, *Phys. Dark Univ.* **5**, 75 (2014) [arXiv:1303.3787]; K. Sato and J. Yokoyama, *Int. J. Mod. Phys. D* **24**, no. 11, 1530025 (2015).
 - [2] G. Lazarides, *Lect. Notes Phys.* **592**, 351 (2002) [hep-ph/0111328]; G. Lazarides, *J. Phys. Conf. Ser.* **53**, 528 (2006) [hep-ph/0607032].
 - [3] G. Dvali, Q. Shafi, and R.K. Schaefer, *Phys. Rev. Lett.* **73**, 1886, 1994 [hep-ph/9406319]; G. Lazarides, R.K. Schaefer, and Q. Shafi, *Phys. Rev. D* **56**, 1324 (1997) [hep-ph/9608256]; G. Lazarides and N.D. Vlachos, *Phys. Rev. D* **56**, 4562 (1997)

- [hep-ph/9707296]; G. Lazarides, *NATO Sci. Ser. II* **34**, 399 (2001) [hep-ph/0011130].
- [4] W. Buchmüller, V. Domcke, and K. Schmitz, *Nucl. Phys.* **B862**, 587 (2012) [arXiv:1202.6679].
- [5] G.R. Dvali, G. Lazarides, and Q. Shafi, *Phys. Lett. B* **424**, 259 (1998) [hep-ph/9710314].
- [6] B. Kyae and Q. Shafi, *Phys. Lett. B* **635**, 247 (2006) [hep-ph/0510105]; M.M.A. Abid, M. Mehmood, M.U. Rehman, and Q. Shafi, *J. Cosmol. Astropart. Phys.* **10**, 015 (2021) [arXiv:2107.05678].
- [7] Y. Akrami *et al.* [Planck Collaboration], *Astron. Astrophys.* **641**, A10 (2020) [arXiv:1807.06211].
- [8] C. Panagiotakopoulos, *Phys. Lett. B* **459**, 473 (1999) [hep-ph/9904284]; C. Panagiotakopoulos, *Phys. Rev. D* **71**, 063516 (2005) [hep-ph/0411143].
- [9] M. Bastero-Gil, S.F. King, and Q. Shafi, *Phys. Lett. B* **651**, 345 (2007) [hep-ph/0604198]; B. Garbrecht, C. Pallis, and A. Pilatsis, *J. High Energy Phys.* **12**, 038 (2006) [hep-ph/0605264]; M.U. Rehman, V.N. Şenoğuz, and Q. Shafi, *Phys. Rev. D* **75**, 043522 (2007) [hep-ph/0612023].
- [10] C. Pallis, *J. Cosmol. Astropart. Phys.* **04**, 024 (2009) [arXiv:0902.0334].
- [11] M.U. Rehman, Q. Shafi, and J.R. Wickman, *Phys. Rev. D* **83**, 067304 (2011) [arXiv:1012.0309]; M. Civatelli, C. Pallis, and Q. Shafi, *Phys. Lett. B* **733**, 276 (2014) [arXiv:1402.6254].
- [12] V.N. Şenoğuz and Q. Shafi, *Phys. Rev. D* **71**, 043514 (2005) [hep-ph/0412102].
- [13] M.U. Rehman, Q. Shafi, and J.R. Wickman, *Phys. Lett. B* **683**, 191 (2010) [arXiv:0908.3896]; M.U. Rehman, Q. Shafi, and J.R. Wickman, *Phys. Lett. B* **688**, 75 (2010) [arXiv:0912.4737]; K. Nakayama *et al.*, *J. Cosmol. Astropart. Phys.* **12**, 010 (2010) [arXiv:1007.5152].
- [14] C. Pallis and Q. Shafi, *Phys. Lett. B* **725**, 327 (2013) [arXiv:1304.5202].
- [15] W. Buchmüller, V. Domcke, K. Kamada, and K. Schmitz, *J. Cosmol. Astropart. Phys.* **07**, 054 (2014) [arXiv:1404.1832].
- [16] Q. Shafi and J.R. Wickman, *Phys. Lett. B* **696**, 438 (2011) [arXiv:1009.5340].
- [17] C. Pallis and Q. Shafi, *Phys. Lett. B* **736**, 261 (2014) [arXiv:1405.7645].
- [18] R. Armillis and C. Pallis, “Recent Advances in Cosmology”, edited by A. Travena and B. Soren (Nova Science Publishers Inc., New York, 2013) [arXiv:1211.4011].
- [19] N. Aghanim *et al.* [Planck Collaboration], *Astron. Astrophys.* **641**, A6 (2020) [arXiv:1807.06209].
- [20] P.A.R. Ade *et al.* [BICEP and Keck], *Phys. Rev. Lett.* **127**, no.15, 151301 (2021) [arXiv:2110.00483].
- [21] G. Lazarides and C. Pallis, *Phys. Lett. B* **651**, 216 (2007) [hep-ph/0702260].
- [22] N. Okada and Q. Shafi, *Phys. Lett. B* **775**, 348 (2017) [arXiv:1506.01410]; M.U. Rehman, Q. Shafi, and F.K. Vardag, *Phys. Rev. D* **96**, no. 6, 063527 (2017) [arXiv:1705.03693]; G. Lazarides, M.U. Rehman, Q. Shafi, and F.K. Vardag, *Phys. Rev. D* **103**, no. 3, 035033 (2021) [arXiv:2007.01474].
- [23] L. Wu, S. Hu, and T. Li, *Eur. Phys. J. C* **77**, no. 3, 168 (2017) [arXiv:1605.00735].
- [24] W. Buchmüller, L. Covi, and D. Delepine, *Phys. Lett. B* **491**, 183 (2000) [hep-ph/0006168].
- [25] S. Antusch, M. Bastero-Gil, K. Dutta, S.F. King, and P.M. Kostka, *J. Cosmol. Astropart. Phys.* **01**, 040 (2009) [arXiv:0808.2425].
- [26] T. Higaki, K.S. Jeong, and F. Takahashi *J. High Energy Phys.* **12**, 111 (2012) [arXiv:1211.0994].
- [27] P. Brax, C. van de Bruck, A.C. Davis, and S.C. Davis, *J. Cosmol. Astropart. Phys.* **09**, 012 (2006) [hep-th/0606140]; S. C. Davis and M. Postma, *J. Cosmol. Astropart. Phys.* **04**, 022 (2008) [arXiv:0801.2116]; S. Mooij and M. Postma, *J. Cosmol. Astropart. Phys.* **06**, 012 (2010) [arXiv:1001.0664].
- [28] C. Pallis, *Phys. Rev. D* **100**, no. 5, 055013 (2019) [arXiv:1812.10284]; C. Pallis, *Eur. Phys. J. C* **81**, no. 9, 804 (2021) [arXiv:2007.06012].
- [29] P.A.R. Ade *et al.* [Planck Collaboration], *Astron. Astrophys.* **594**, A13 (2016) [arXiv:1502.01589].
- [30] W. Buchmüller, V. Domcke, and K. Schmitz, arXiv:2307.04691; S. Antusch, K. Hinze, S. Saad, and J. Steiner, arXiv:2307.04595; B. Fu, S.F. King, L. Marsili, S. Pascoli, J. Turner, and Y.-L. Zhou, arXiv:2308.05799; G. Lazarides, R. Maji, M. Moursy, and Q. Shafi, arXiv:2308.07094; A. Afzal, A. Mehmood, M.U. Rehman, and Q. Shafi, arXiv:2308.11410; R. Maji and W.I. Park, arXiv:2308.11439.
- [31] A. Afzal *et al.* [NANOGrav Collaboration], *Astrophys. J. Lett.* **951**, no. 1, L11 (2023) [arXiv:2306.16219].
- [32] G. Agazie *et al.* [NANOGrav Collaboration], *Astrophys. J. Lett.* **951**, no. 1, L8 (2023) [arXiv:2306.16213].
- [33] J. Antoniadis *et al.* [EPTA Collaboration] arXiv:2306.16214; D.J. Reardon *et al.*, *Astrophys. J. Lett.* **951**, no. 1, L6 (2023) [arXiv:2306.16215]; H. Xu *et al.*, *Res. Astron. Astrophys.* **23**, no. 7, 075024 (2023) [arXiv:2306.16216].
- [34] R. Abbott *et al.* [LIGO Scientific, Virgo, and KAGRA Collaboration], *Phys. Rev. Lett.* **126**, no. 24, 241102 (2021) [arXiv:2101.12248].
- [35] K.J. Bae, H. Baer, V. Barger, and D. Sengupta, *Phys. Rev. D* **99**, no. 11, 115027 (2019) [arXiv:1902.10748].
- [36] G.F. Giudice and A. Masiero, *Phys. Lett. B* **206**, 480 (1988).
- [37] A. Brignole, L.E. Ibáñez, and C. Muñoz, *Adv. Ser. Direct. High Energy Phys.* **18**, 125 (1998) [hep-ph/9707209].
- [38] G. Kane, K. Sinha, and S. Watson, *Int. J. Mod. Phys. D* **24**, no. 08, 1530022 (2015) [arXiv:1502.07746].
- [39] K.J. Bae, H. Baer, V. Barger, and R.W. Deal, *J. High Energy Phys.* **02**, 138 (2022) [arXiv:2201.06633].
- [40] M. Endo, F. Takahashi, and T.T. Yanagida, *Phys. Rev. D* **76**, 083509 (2007) [arXiv:0706.0986].
- [41] J. Ellis, M. Garcia, D. Nanopoulos, and K. Olive, *J. Cosmol. Astropart. Phys.* **10**, 003 (2015) [arXiv:1503.08867].
- [42] Y. Aldabergenov, I. Antoniadis, A. Chatrabhuti, and H. Isono, *Eur. Phys. J. C* **81**, no. 12, 1078 (2021) [arXiv:2110.01347].
- [43] T. Hasegawa *et al.*, *J. Cosmol. Astropart. Phys.* **12**, 012 (2019) [arXiv:1908.10189].
- [44] M. Endo *et al.*, *Phys. Rev. Lett.* **96**, 211301 (2006) [hep-ph/0602061]; S. Nakamura and M. Yamaguchi, *Phys. Lett. B* **638**, 389 (2006) [hep-ph/0602081].
- [45] H. Baer *et al.*, *Eur. Phys. J. ST* **229**, no. 21, 3085 (2020) [arXiv:2002.03013].
- [46] W. Buchmüller, E. Dudas, L. Heurtier, and C. Wieck, *J. High Energy Phys.* **14**, 053 (2014) [arXiv:1407.0253]; E. Dudas, T. Gherghetta, Y. Mambrini, and K.A. Olive, *Phys. Rev. D* **96**, no. 11, 115032 (2017) [arXiv:1710.07341].
- [47] J. Ellis, D.V. Nanopoulos, K.A. Olive, and S. Verner, *Phys. Rev. D* **100**, no. 2, 025009 (2019) [arXiv:1903.05267]; J. Ellis, D. V. Nanopoulos, K. A. Olive, and S. Verner, *J. Cosmol. Astropart. Phys.* **08**, 037 (2020) [arXiv:2004.00643].
- [48] I. Antoniadis, A. Chatrabhuti, H. Isono, and R. Knoop, *Eur. Phys. J. C* **76**, no. 12, 680 (2016) [arXiv:1608.02121]; Y. Aldabergenov, A. Chatrabhuti, and S.V. Ketov, *Eur. Phys. J. C* **79**, no. 8, 713 (2019) [arXiv:1907.10373]; I. Antoniadis, O. Lacombe, and G.K. Leontaris, *Eur. Phys. J. C* **80**, no. 11,

- 1014 (2020) [arXiv:2007.10362]; Y. Aldabergenov, A. Chababuti, and H. Isono, *Eur. Phys. J. C* **81**, no. 2, 166 (2021) [arXiv:2009.02203].
- [49] V. Domcke and K. Schmitz, *Phys. Rev. D* **95**, no. 7, 075020 (2017) [arXiv:1702.02173]; V. Domcke and K. Schmitz, *Phys. Rev. D* **97**, no. 11, 115025 (2018) [arXiv:1712.08121].
- [50] M.C. Romão and S.F. King, *J. High Energy Phys.* **07**, 033 (2017) [arXiv:1703.08333]; S.F. King and E. Perdomo, *J. High Energy Phys.* **05**, 211 (2019) [arXiv:1903.08448].
- [51] R. Kallosh and A. Linde, *Phys. Rev. D* **91**, 083528 (2015) [arXiv:1502.07733]; A. Linde, *J. Cosmol. Astropart. Phys.* **11**, 002 (2016) [arXiv:1608.00119].
- [52] G. Aad *et al.* [ATLAS Collaboration], *Phys. Rev. D* **90**, 052004 (2014); CMS Collaboration, Tech. Rep. CMS-PAS-HIG-14-009 (2014).
- [53] E. Bagnaschi, G.F. Giudice, P. Slavich, and A. Strumia, *J. High Energy Phys.* **09**, 092 (2014) [arXiv:1407.4081].
- [54] R. Jeannerot, S. Khalil, G. Lazarides, and Q. Shafi, *J. High Energy Phys.* **10**, 012 (2000) [hep-ph/0002151]; R. Jeannerot, S. Khalil, and G. Lazarides, *J. High Energy Phys.* **07**, 069 (2002) [hep-ph/0207244].
- [55] G. Lazarides and C. Panagiotakopoulos, *Phys. Rev. D* **52**, R559 (1995) [hep-ph/9506325]; G. Lazarides and A. Vamvasakis, *Phys. Rev. D* **76**, 083507 (2007) [arXiv:0705.3786]; M.U. Rehman and Q. Shafi, *Phys. Rev. D* **86**, 027301 (2012) [arXiv:1202.0011].
- [56] P. Binétruy, *Supersymmetry: Theory, experiment and cosmology*, Oxford (2006).
- [57] G. Lazarides and Q. Shafi, *Phys. Rev. D* **58**, 071702 (1998) [hep-ph/9803397].
- [58] C. Pallis, *Astropart. Phys.* **21**, 689 (2004) [hep-ph/0402033]; C. Pallis, *Nucl. Phys.* **B751**, 129 (2006) [hep-ph/0510234].
- [59] M. Hindmarsh, *Prog. Theor. Phys. Suppl.* **190**, 197 (2011) [arXiv:1106.0391].
- [60] M. Mehmood, M.U. Rehman, and Q. Shafi, *J. High Energy Phys.* **02**, 181 (2021) [arXiv:2010.01665]; J. Ellis, J.L. Evans, N. Nagata, D.V. Nanopoulos, and K.A. Olive, *Eur. Phys. J. C* **81**, no. 12, 1109 (2021) [arXiv:2110.06833].
- [61] Y. Cui, M. Lewicki, D.E. Morrissey, and J.D. Wells, *J. High Energy Phys.* **01**, 081 (2019) [arXiv:1808.08968]; P. Auclair *et al.*, *J. Cosmol. Astropart. Phys.* **04**, 034 (2020) [arXiv:1909.00819]; Y. Gouttenoire, G. Servant, and P. Simakachorn, *J. Cosmol. Astropart. Phys.* **07**, 032 (2020) [arXiv:1912.02569].
- [62] M.M. Flores, A. Kusenko, L. Pearce, and G. White, arXiv:2208.09789.
- [63] J. Garcia-Bellido *et al.*, *Phys. Rev. D* **60**, 123504 (1999) [hep-ph/9902449]; L.M. Krauss and M. Trodden, *Phys. Rev. Lett.* **83**, 1502 (1999) [hep-ph/9902420].